Ranking number:

Serial Number:

People's Democratic Republic of Algeria

Ministry of Higher Education and Scientific Research

University of Shahid Hamma Lakhdar El Oued

Faculty of Natural and Life Sciences Department of Biology

Graduation Note to obtain

an academic master's degree

in the field of natural and life science

Division of Biological Sciences

Specialty of Toxicology

Theme

Synthesis and Characterization of Ni(II) and Zn(II) Porphyrin Complexes: In Vitro and In Silico Evaluation of Anti-Diabetic Potential via ADMET, Molecular Docking, and Dynamics Simulations

Prepared by :

- ATALLAH Hadjer
- BARKA chourouk
- BEKAKRA salem
- ADOUKA Teber

Jury members :

- President:
- Co- Supervisor: Dr. LANEZ Elhafnaoui El_Oued University
- Primary Supervisor:BEN AMORMohmmed Larbi
- Examiner:

Academic year: 2024/2025

شكر وتقدير

الشكر أولاً إلى الله عز وجل، القائل في محكم كتابه العزيز:

{لَئِن شَكَرْتُمْ لَأَزِيدَنَّكُمْ} [إبراهيم:7]

فالحمد لله الذي وهبنا نعمة العقل، لينير لنا الطريق، ووفقنا بمشيئته وقدرته لإتمام هذا العمل وبلوغه هذه الصورة.

وإنّ من تمام الوفاء والعرفان، أن نرفع أسمى عبارات الشكر والتقدير لكل من مدّ لنا يد العون، وساهم في إنجاز هذا البحث، ولو بكلمة أو رأي أو توجيه صادق.

نخصّ بالشكر والتقدير:

الدكتور العانز الحفناوي، على إشرافه الكريم على هذا العمل، وما قدّمه لنا من دعم وتوجيهات علمية كان لها بالغ الأثر في إتمام هذا البحث.

كما نتقدّم بجزيل الشكر إلى:

الدكتور بن عمر العربي، على ملاحظاته البنّاءة ونصائحه القيمة التي أثْرت محاور البحث.

وإلى **الأستاذة الفاضلة عائشة عدائكة،** التي رافقتنا في الجانب التطبيقي، وساهمت بإشرافها ودعمها داخل المخبر في تذليل العقبات وإنجاز العمل العملي بالشكل الأمثل.

نسأل الله أن يجعل هذا الجهد خالصًا لوجهه الكريم، نافعًا لنا ولغيرنا، وأن يبارك في كل من أسهم في إنجاز هذا العمل، ودعَمنا بكلمة، أو وقت، أو توجيه

الإهداء

قال تعالى:

(يرفع الله الذين آمنوا منكم والذين أوتوا العلم درجات والله بما تعملون خبير) سورة المجادلة. الآية رقم 11

الحمدلله الذي بنعمته تتم الصالحات. أخيراً تحقق حلم التخرج. لطالما انتظرت هذا اليوم كي ارى الفخر والسعادة في عين أمي وأبي. وها أنا اليوم اهدي تخرجي الى :

"أبي الحبيب"الذي علمني أن النجاح لا يأتي إلا بالجد والاجتهاد، والذي كان لي القدوة والمثل الأعلى في الصبر والمثابرة، إليك يا من كنت لي الصديق والموجه، ولم تتوانَ يومًا عن تقديم النصيحة والدعم لي في كل مراحل حياتي.

أقول لك: شكرًا من القلب على كل ما قدمته لي، وعلى كل لحظة قضيتها في دعمي وتشجيعي، أهديك هذا البحث الذي لولاك ما كنت ولا كان.

الى نبع الحنان و القلب الناصع بالبياض من تستقبلني بابتسامه و تودعني بدعوه "امي الغاليه"التي كانت لي الام الحنون و المعلمه الاولى و التي غرست في نفسي القيم و المبادئ و التي كانت لي السند في كل الاوقات من كانت لي الملاذ الامن و التي سعت في تقديم الحب و الحنان لي. اطال الله في عمركما وجعلكما خيمة فوق رؤوسنا.

الى من هم انس عمري ومخزن ذكرياتي اخواني"حمزه' الصادق'شعيب"واخواتي الحبيبات.
بالذكر صديقاتي العزيزات اخص كما لا يفوتني ان"هاجر 'اسماء 'خلود"

والى كل الاشخاص الذين احمل لهم المحبة و التقدير.

شروق

الإهداء

وتتمنى ألّا يكون طريقك وعراً لتنجو، فيكون طريقك وعراً وتنجو... لتعلم أن النجاة من الله، لا من الطريق.

"لم تكن الرحلة قصيرة، ولا ينبغي لها أن تكون... لم يكن الحلم قريبًا، ولا الطريق كان محفوفاً بالتسهيلات لكنني فعلتها... ونلتها.

إلى من دعمني بلا حدود، علّمني أن الحياة كفاح، وسلاحي فيها العلم والأخلاق، إلى فخري وسندي بعد الله..."والدي العزيز".

وإلى من كانت دعواتها بردًا وسلامًا، من احتواني قلبها قبل يدها، إلى وهج حياتي..." والدتي الغالية".

إلى إخوتي وأخواتي الأحبة :

"معمر، عبد الرزاق، العيد، إسحاق، عائشة، خديجة، وسارة" كنتم الضلع الثابت، والسند الذي لا يميل.

إلى زوجات أخي "مريم وعفاف" بروحكما الطيبة، كنتما نعم الأخوات.

إلى فلذات الأكباد، بهجتي وسر سعادتي:

"داوود، ميرال، قصي، نضال، أنس، هديل، يزن، ورتيل".

إلى صديقات القلب، رفيقات الدرب...

كنتنّ النور حين أظلمت الأيام، ، وأخصّ" خديجة وشيماء"... أنتما الأثر الذي لا يُمحى.

وإلى فلسطين... أرض الفداء، وشهداؤها الأكرم منا، وأسرانا الأحرار... لكم في القلب دعاء لا ينقطع.

لكل من ساندني في هذا الطريق، أهديكم ثمرة هذا الجهد، راجية من الله أن ينفعني بما تعلمت، ويجعله حجة لي لا عليّ.

تبر

الإهداء

الحمد لله حبا كثيرا و امتنانا على البدء و على الختام (وآخر دعواهم أن الحمد لله رب العالمين)

إهداء إلى" روح أبي الغالية"،إلى من رحل عن الدنيا، وبقي حيًّا في قلبي،إلى من علّمني القوة، وغرس في قلبي القيم

رحمك الله وجعل .والمبادئ، نم قرير العين يا أبي، فدعاؤك لا يفارق لساني، وذكراك تسكن وجداني مثواك الجنة.

سالم

الإهداء

اهدي ثمرة جهدي هذا :

إلى من كان دعاؤها سندي، وصبرها ،قوتي وحنانها دوائي.... إلى "أمي الحبيبة"، التي لولاها لما وصلت إلى ما أنا عليه

إلى "أبي العزيز"، الذي علمني معنى الاجتهاد، وغرس في نفسي حب العلم.

إلى إخوتي وأخواتي، سندي الدائم، ومصدر قوتي.

إلى كل من ساندني بكلمة، بدعاء، أو بابتسامة

هاجر

Résumé

Dans cette recherche, nous avons étudié l'effet des porphyrines en tant qu'inhibiteurs de l'α-amylase, une enzyme clé dans la digestion des glucides, afin d'améliorer le contrôle du taux de glucose sanguin chez les patients diabétiques. Quatre composés dérivés de la porphyrine (P1-P4) ont été testés, et les résultats ont montré que le composé P4 était le plus efficace pour inhiber l'α-amylase, enregistrant la plus faible valeur d'IC50 (0,004 µg/mL). Le composé P2 a également montré une forte activité inhibitrice (IC50 = 0,016 µg/mL), tandis que les autres composés étaient moins efficaces.

Nous avons également utilisé des calculs de chimie quantique (DFT) pour étudier les propriétés de ces composés, révélant que $NiPPH_2$ et $ZnTPPH_2$ possèdent des caractéristiques chimiques favorables à leur activité biologique. De plus, une simulation moléculaire a été réalisée pour mieux comprendre les interactions entre les composés et l'enzyme α-amylase.

Les résultats suggèrent que les porphyrines, en particulier les composés P4 et P2, possèdent un fort potentiel d'inhibition de l'α-amylase, ce qui pourrait contribuer à une meilleure régulation de la glycémie. Il est recommandé de poursuivre les recherches pour évaluer la toxicité, le métabolisme et l'efficacité clinique de ces composés.

Mots-clés :

Porphyrine, α-Amylase,Diabète de type 2,Inhibition enzymatique,In Vitro,In Silico,Docking moléculaire,CI50,Composés naturels,Régulation de la glycémie.

Abstract:

In this study, we investigated the effect of porphyrins as inhibitors of α-amylase, a key enzyme in carbohydrate digestion, with the aim of improving blood glucose control in diabetic patients. Four porphyrin-derived compounds (P1–P4) were tested, and the results showed that compound P4 was the most effective in inhibiting α-amylase, recording the lowest IC50 value (0.004 µg/mL). Compound P2 also demonstrated strong inhibitory activity (IC50 = 0.016 µg/mL), while the other compounds were less effective.

We also used quantum chemical calculations (DFT) to study the properties of these compounds, revealing that $NiPPH_2$ and $ZnTPPH_2$ have chemical characteristics that support their biological activity. Additionally, molecular docking simulations were conducted to better understand the interactions between the compounds and the α-amylase enzyme.

The results suggest that porphyrins, especially compounds P4 and P2, have great potential in inhibiting α-amylase, which could help improve blood sugar control. Further studies are recommended to assess the toxicity, metabolism, and clinical efficacy of these compounds.

Keywords:

Porphyrin, α-Amylase, Type 2 Diabetes, Enzyme Inhibition, In Vitro,In Silico; Molecular Docking, IC50, Natural Compounds, Blood Glucose Regulation.

ملخص

في هذا البحث، قمنا بدراسة تأثير البورفيرينات كمثبطات لإنزيم الألفا-أميلاز، وهو إنزيم رئيسي في هضم الكربوهيدرات، بهدف تحسين التحكم في مستويات الجلوكوز في الدم لمرضى السكري. تم اختبار أربع مركبات مشتقة من البورفيرين (P1-P4)، وأظهرت النتائج أن المركب P4 كان الأكثر فعالية في تثبيط الألفا-أميلاز، حيث سجل أدنى قيمة لـ IC50=0.004 (ميكروغرام/مل). كما أظهر المركب P2 أيضًا نشاطًا مثبطًا قويًا IC50=0.016 (ميكروغرام/مل)، بينما كانت المركبات الأخرى أقل فعالية.

استخدمنا أيضًا الحسابات الكيميائية الكمومية (DFT) لدراسة خصائص هذه المركبات، وأظهرت النتائج أن المركبات $NiPPH_2$ و $ZnTPPH_2$ تتمتع بخصائص كيميائية تدعم نشاطها البيولوجي. بالإضافة إلى ذلك، تم إجراء محاكاة جزيئية لفهم التفاعلات بين المركبات وإنزيم الألفا-أميلاز.

النتائج تشير إلى أن البورفيرينات، وخاصة المركبات P4 وP2، لها إمكانيات كبيرة في تثبيط الألفا-أميلاز، مما يمكن أن يساعد في تحسين التحكم في مستويات السكر في الدم. ننصح بإجراء مزيد من الدراسات لتقييم السمية والتمثيل الغذائي للمركبات، بالإضافة إلى دراسات سريرية لتقييم فعاليتها وسلامتها في البشر.

الكلمات المفتاحية:

بورفيرين، إنزيم الألفا-أميليز، السكري من النوع الثاني،تثبيط الإنزيم، في المختبر (In Vitro)،محاكاة حاسوبية (In Silico)، الالتحام الجزيئي، قيمةIC50،المركبات الطبيعية، تنظيم سكر الدم

SUMMARY

Chapter 2 DIABETES

List of figures

List of tables

GENERAL INTRODUCTION

Introduction

Diabetes mellitus is a chronic metabolic disorder characterized by persistent hyperglycemia (elevated blood glucose levels), which arises from defects in insulin secretion, insulin action, or both. This condition affects millions of people worldwide and has become a global public health concern due to its association with severe complications such as cardiovascular diseases, kidney failure, neuropathy, and vision loss. The global rise in the incidence of diabetes is linked to factors such as an aging population, poor dietary habits, sedentary lifestyles, and genetic predispositions. Effective management of diabetes is crucial for preventing these complications, and current treatment strategies primarily focus on insulin therapy and oral hypoglycemic agents. However, the limitations of existing treatments, such as adverse effects, the need for constant monitoring, and the lack of curative solutions, have prompted researchers to explore new therapeutic alternatives.

In this context, natural and synthetic compounds have been extensively studied for their potential to prevent or manage diabetes. Among these, porphyrins, a class of heterocyclic macrocyclic compounds, have garnered significant attention due to their unique chemical structure and versatile biological activities. Porphyrins are characterized by a porphine ring system, which is responsible for their redox properties and ability to undergo various chemical reactions. This structure allows them to participate in biological processes such as electron transfer, antioxidant activity, and enzyme inhibition, which are critical in the management of metabolic diseases like diabetes.

Recent research has increasingly focused on the potential antidiabetic properties of porphyrin derivatives. These compounds are believed to exert their beneficial effects through a variety of mechanisms, including antioxidant, anti-inflammatory, and enzyme-inhibitory actions. Oxidative stress, resulting from an imbalance between reactive oxygen species (ROS) and the body's antioxidant defense mechanisms, plays a significant role in the pathogenesis of diabetes. Porphyrins, with their antioxidant properties, can help counteract oxidative damage, thus protecting pancreatic beta cells from apoptosis and improving insulin secretion and sensitivity.

In addition to their antioxidant effects, some porphyrin derivatives have been found to inhibit enzymes involved in carbohydrate digestion, such as α-amylase and α-glucosidase. These enzymes play a crucial role in breaking down complex carbohydrates into simpler

sugars, which are then absorbed into the bloodstream. By inhibiting these enzymes, porphyrins can help reduce postprandial blood sugar spikes, thereby improving overall glycemic control. Furthermore, porphyrins have shown promise in modulating inflammatory pathways that contribute to insulin resistance, another hallmark of diabetes.

Given these diverse mechanisms of action, porphyrins represent a promising avenuefor the development of novel therapeutic agents for the treatment or management of diabetes mellitus. Their potential to reduce oxidative stress, improve insulin sensitivity, and inhibit carbohydrate-digesting enzymes positions them as valuable candidates for advancing diabetic care. With further research and clinical testing, porphyrins and their derivatives may play a pivotal role in shaping future diabetes management strategies.

FIRST PARTTHE ORETICAL PART

CHAPTER I

Bibliographic study of porphyrins

1. General Information on porphyrins:

1. Definition, properties and applications of porphyrins :

Porphyrin is a large macrocyclic molecule consisting of four pyrrole units connected by methene bridges. These bridges define the four meso positions of the porphyrin ring, while the carbon atoms within the pyrrole rings form the α and β positions (see Figure1). The porphyrin structure contains a total of 22 π electrons, 18 of which are delocalized and contribute to its aromatic character. This aligns with Hückel's rule, which states that aromatic systems must contain 4n + 2 delocalized π electrons—where n in this case equals 4. The fully unsubstituted form of porphyrin is called porphine.

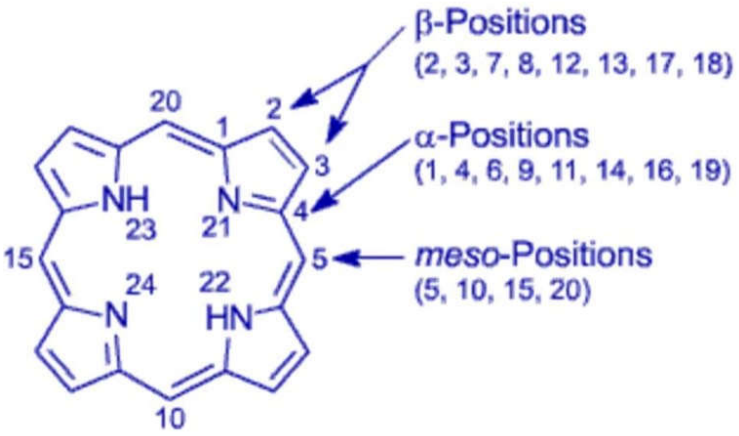

Figure1. Structure of porphine

Porphyrin can be found in the so-called 'freebase' form (Figure1) or in a metal-complexed form, wherein a metal cation, typically with an oxidation state of (+II) or (+III), is coordinated (Figure 2). [1]

Figure2. Metalized porphine

2. Spectroscopic and electrochemical characterizations of porphyrins:

2.1. NMR nuclear magnetic resonance:

2.1.1. Proton NMR spectroscopy (1H NMR)

When proton NMR spectroscopy is applied to porphyrin macrocycles, two distinct types of signals are typically observed, corresponding to the protons at the meso, α, and β positions.

The β-pyrrolic protons generally appear in the downfield region around 8–9 ppm. The multiplicity and pattern of these signals are influenced by the symmetry of the porphyrin molecule and the nature of the substituents at the meso positions.

Protons attached to the pyrrolic nitrogen atoms usually resonate at around -2 ppm. These signals are broad and exchangeable, due to their involvement in dynamic proton exchange processes [2].

The aromatic nature of the porphyrin ring creates a strong ring current when placed in a magnetic field. This results in significant magnetic anisotropy, generating a shielding cone perpendicular to the plane of the macrocycle. Protons located inside this cone, such as those bonded to pyrrolic nitrogen atoms, are strongly shielded and resonate upfield (around -2 to 3 ppm). In contrast, the β-pyrrolic protons outside the cone experience strong deshielding, leading to downfield shifts (8–9 ppm).

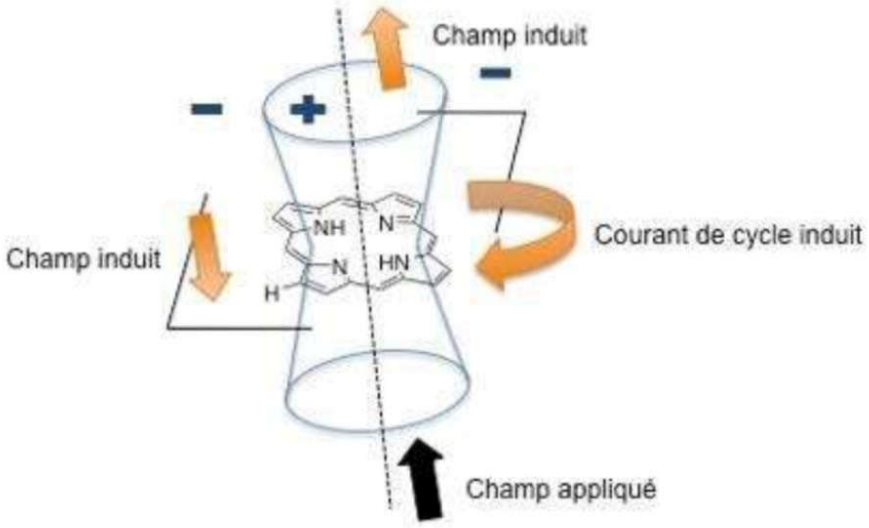

Figur3. Anisotropy magnetic cone of a porphyrin

The ^{1}H NMR spectrum of porphine, which is the unsubstituted form of porphyrin, displays three distinct singlet signals at chemical shifts of -3.76, 9.74, and 10.50 ppm [4]. These peaks correspond respectively to the protons bonded to the inner nitrogen atoms, the β-pyrrolic protons, and the methine (meso) protons. The methine protons, being attached to electron-deficient carbon atoms, experience greater deshielding than the β-pyrrolic protons, which explains their appearance further downfield. Additionally, the singular nature of the β-pyrrolic proton signal is attributed to the rapid tautomeric exchange involving the inner NH protons [5], as illustrated in Figure 1.4.

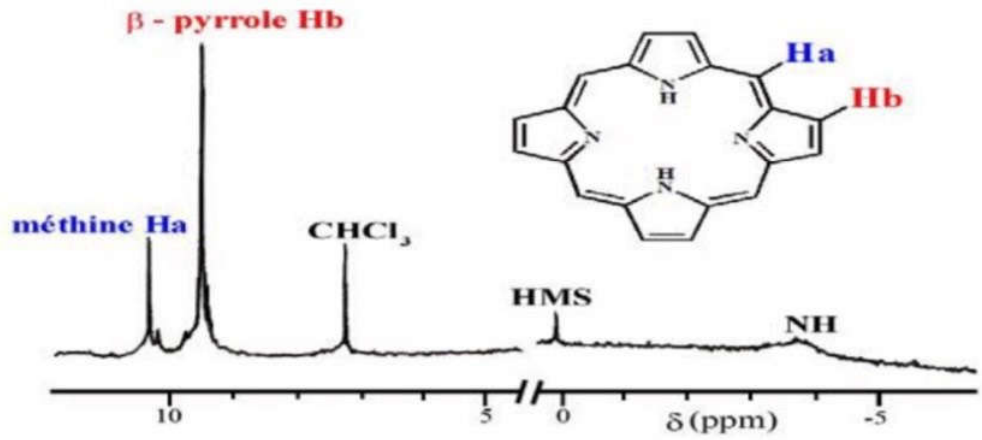

Figure4.1H NMR spectrum of porphyrin in CHCl3

2.1.2. Carbon-13 NMR Spectroscopy (13C NMR) :

The ^{13}C NMR spectrum of porphyrins typically reveals signals corresponding to three distinct types of carbon atoms: α-pyrrolic, β-pyrrolic, and meso carbons. However, identifying the signals of the α and β carbons can be challenging due to the presence of NH tautomerism, which causes signal broadening and overlap. This tautomerism slows down at lower temperatures, making the carbon signals more distinguishable under such conditions.

Generally, α-carbons resonate around 145 ppm, and their signals exhibit a relatively consistent chemical shift difference of approximately 17 ppm. β-carbons typically appear around 130 ppm, with a smaller chemical shift variation ranging between 5.3 and 6.9 ppm.

Meso carbon atoms, on the other hand, are usually observed between 95 and 120 ppm. Upon metallation of the porphyrin core, the signals of α and β carbons tend to shift upfield, whereas meso carbon signals are shifted downfield [6].

2.2. UV-Visible Spectroscopy :

The UV-visible spectrum of porphyrins is characterized by two main absorption regions, resulting from distinct electronic transitions within their extensively conjugated π-electron system [7]. This high degree of conjugation enables porphyrins to absorb within the visible range, producing a distinctive absorption profile.

The most intense absorption band, known as the Soret band (or B band), occurs between 390 and 430 nm in the near-UV region. It is attributed to $\pi \rightarrow \pi^*$ electronic transitions and is characterized by a high molar extinction coefficient, typically exceeding 100,000 $L \cdot mol^{-1} \cdot cm^{-1}$ [8].

In addition to the Soret band, four less intense bands appear in the visible region, spanning from 480 to 700 nm. These are referred to as Q bands and exhibit absorption intensities that are approximately 10 to 20 times lower than the Soret band. The Q bands, labeled I to IV in order of increasing energy, are particularly sensitive to structural changes within the porphyrin macrocycle.

Modifications such as substitution at various positions on the ring can significantly influence the number, position, and intensity of the Q bands, providing valuable information about the porphyrin structure [9].

Based on these variations, four general spectral types have been identified: etio, rhodo, oxorhodo, and phyllo.[10]

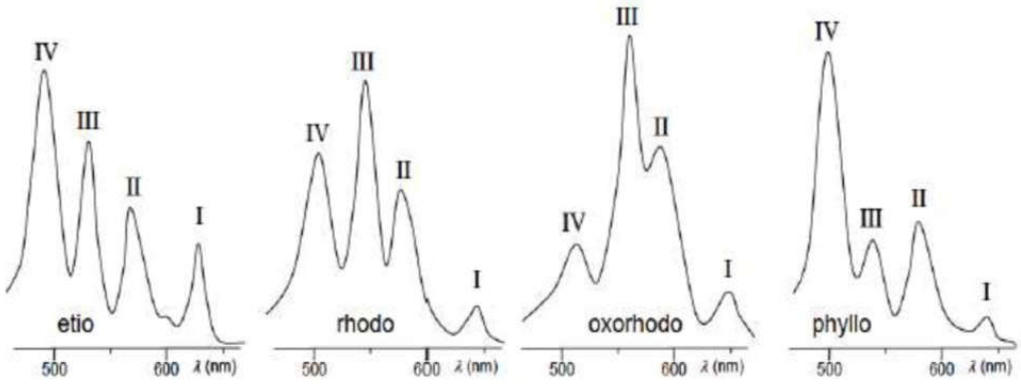

Figure5. Different Q bands of free base porphyrins

2.3. Cyclic Voltammetry:

The electrochemical behavior of porphyrins is influenced by several factors, including whether the porphyrin exists as a free base or metal complex, the nature of the substituents on the macrocyclic ring, and the solvent used during analysis. Among the most extensively studied porphyrins is tetraphenylporphyrin (TPP).

Cyclic voltammetry of free-base porphyrins typically reveals two distinct single-electron oxidation processes and between two to four single-electron reduction steps [11–14]. The first oxidation step leads to the formation of a radical cation [15], which is further oxidized into a dication in the second step. During the reduction process, a radical anion is initially produced, followed by the formation of a dianion after the second reduction.

The electrochemical reduction of TPP, in particular, shows that the third and fourth reduction steps involve more complex behavior and mechanisms [16,17]. The radical cations generated during the first oxidation of free-base porphyrins are known to be highly reactive, often resulting in protonation of the porphyrin ring [18].

In 1998, Yves Le Mest and his team proposed a mechanistic pathway for the protonation of TPP during the oxidation process (see Scheme1). Their findings indicated that the monoprotonated form of TPP is unstable, and the final deprotonated product forms after the loss of two electron equivalents. It is believed that the hydrogen radicals involved in this process originate from the solvent used during the experiment.

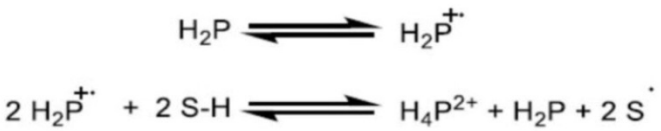

Schema1.proposed mechanisms for the protonation of TPP during their first-stage oxidation.

In metalloporphyrins containing non-electroactive metal cations—such as Zn(II) or Mg(II)—the redox behavior observed via cyclic voltammetry closely resembles that of free-base porphyrins. While the metal center does not directly participate in redox processes, it significantly influences the oxidation and reduction potentials of the macrocyclic ring. These redox potentials are strongly dependent on the electronegativity of the incorporated metal [19]. In general, a higher metal electronegativity facilitates oxidation while making reduction more difficult [20].In the 1970s, Fuhrhop and his colleagues reported that the potential difference between the first oxidation and the first reduction of a porphyrin macrocycle ($\Delta|Red_1–Ox_1|$) is approximately 2.25 ± 0.15 V. They also found that the first and second

oxidation events are typically separated by a potential gap of about 0.3 ± 0.1 V ($\Delta|Ox_2–Ox_1|$), while the first and second reductions are separated by approximately 0.4 ± 0.1 V ($\Delta|Red_2–Red_1|$) [14], as illustrated in Figure I.6. It is important to note that these electrochemical characteristics are valid only for porphyrins complexed with non-electroactive metal centers.

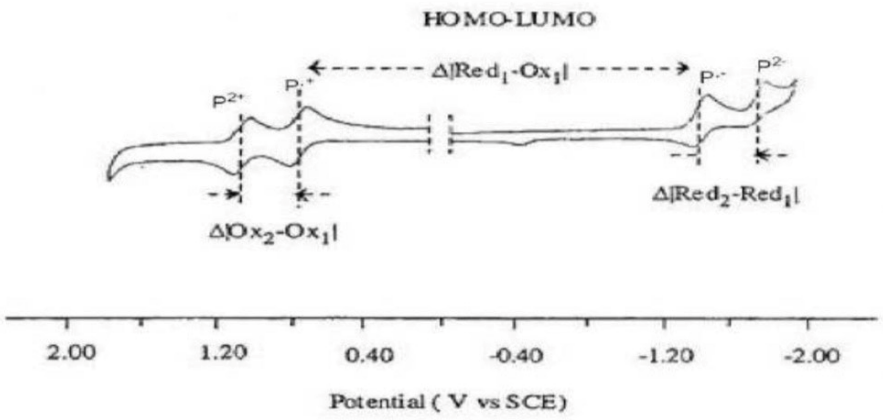

Figure1. Cyclic voltammetry of TPP in CH2Cl2.

3. Description of porphyrin synthesis pathways :

Porphyrins are typically synthesized through the condensation reaction between pyrrole and an aldehyde in the presence of an acid catalyst and an oxidizing agent, following the classical Rothemund method. Extensive research has been devoted to the synthesis of porphyrins bearing substituents at the meso and/or β positions of the porphine ring. In particular, numerous studies have focused on elucidating the mechanism underlying porphyrin formation.

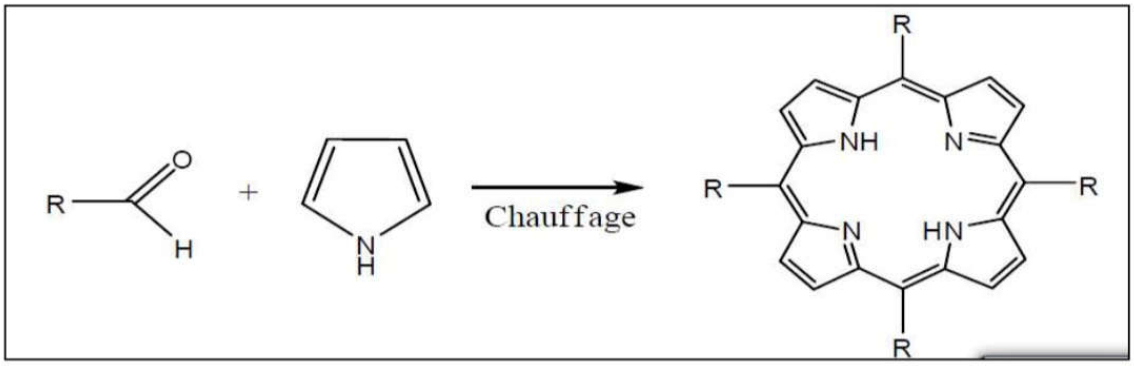

Figure2. Method of Rothemund

Tetraphenylporphyrin (TPP) is among the most extensively studied porphyrins. Its synthesis, as initially established by Adler and Longo in 1967, is influenced by several parameters, including the acidity of the medium, choice of solvent, reaction temperature, oxygen availability, and the initial concentrations of the reactants. Through systematic studies, the most efficient synthetic route was identified: the condensation of four equivalents of pyrrole with benzaldehyde under reflux in propionic acid at 141°C. This method consistently yields TPP in crystalline form with an average yield of approximately 20% [21–24].

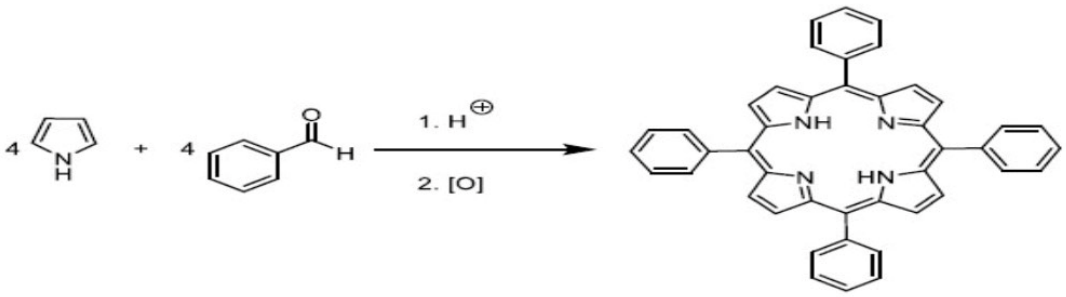

Figure3. Method of Adler and Longo

Lindsey and his collaborators introduced significant improvements to the original method developed by Adler and Longo [25–28]. In this approach, pyrrole is condensed with an aldehyde in a chlorinated solvent such as dichloromethane or chloroform, using a catalytic amount of trifluoroacetic acid (TFA) or boron trifluoride etherate ($BF_3 \cdot Et_2O$) at room temperature. The intermediate porphyrinogen formed during the reaction is subsequently oxidized using an oxidizing agent like 2,3-dichloro-5,6-dicyano-1,4-benzoquinone (DDQ), resulting in the formation of meso-tetrasubstituted porphyrins with yields ranging from 30% to 40%.

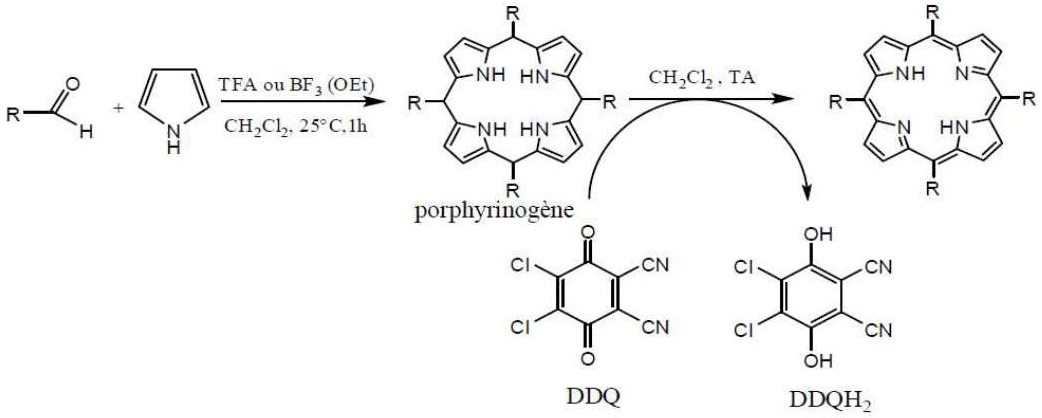

Figure9. Method of Lindsey

MacDonald proposed a more directed synthetic strategy involving a three-step process [29], as depicted in Figure10. The initial step entails the formation of dipyrromethane through the reaction of an aldehyde with an excess of pyrrole. Alternatively, a [2+2] condensation can be carried out using various aldehydes and dipyrromethanes, following MacDonald's methodology [30].

However, a major limitation of this approach is the generation of statistical mixtures of isomers. These mixtures are often difficult to separate and purify, leading to reduced overall yields, especially when a specific isomer is desired [31]

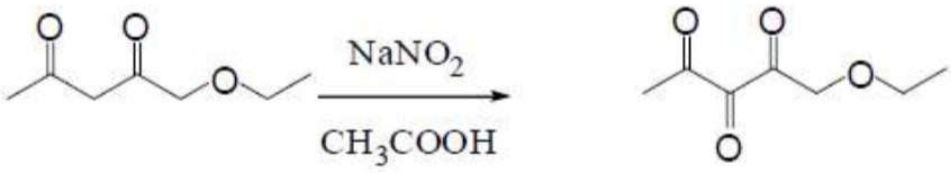

Figure10. Method Mac Donald

The introduction of functional groups at the β-pyrrolic positions is typically achieved through the preparation of pre-functionalized pyrrolic intermediates. These intermediates include basic pyrroles, such as dipyrromethanes, and more complex structures like α,β-diladienes, which are oligomeric forms of four pyrrole units. By systematically incorporating

various functional groups under controlled conditions, modified porphyrin derivatives can be synthesized[32]

One notable method for synthesizing functionalized pyrroles is the Knorr method, which produces highly functionalized pyrroles from simple substrates. Developed in 1884, this method involves the stoichiometric reaction of ethyl acetoacetate with an oxime, prepared by treatment with sodium nitrite, followed by reduction with zinc in acetic acid.(Figure11)

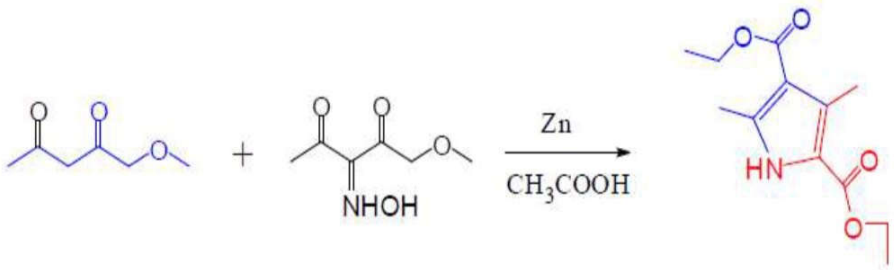

Figure4. Method of Knorr

Another important method for synthesizing pyrroles is the Barton-Zard method. This approach involves the use of nitroacetate, which, after deprotecting the acetate group in the presence of a base, forms a nitroalkane. The nitroalkane then reacts with a derivative of isocyanoacetate, leading to cyclization and the formation of the desired pyrrole, following the elimination of the nitro (NO2) group. [33]

Figure12. Method of Barton-Zard

4. Toxicity of Porphyrins

Porphyrins are widely utilized as photosensitizers in photodynamic therapy (PDT) due totheir ability to generate reactive oxygen species (ROS) upon light activation. This

propertyenables targeted destruction of malignant cells. However, the potential toxicity of porphyrins,both in light and dark conditions, necessitates careful consideration.

In the absence of light (dark toxicity), certain porphyrin derivatives can exhibit cytotoxiceffects. This is often attributed to their physicochemical properties, such as lipophilicity andcharge, which influence their cellular uptake and localization. For instance, cationicporphyrins may interact with cellular membranes or organelles, leading to oxidative stress andcell death even without photoactivation. The degree of dark toxicity is influenced by factors including chemical structure, concentration, and the specific cell type involved

Upon light activation, porphyrins can produce ROS, leading to phototoxic effects. Whilethis is the desired mechanism in PDT, unintended damage to surrounding healthy tissues canoccur if the photosensitizer is not adequately targeted. Therefore, strategies such asconjugation with targeting ligands or encapsulation in nanocarriers have been developed toenhance selectivity and minimize off-target effects.

A study evaluating the toxicity of a porphyrin-based photosensitizer in an in vivo modeldemonstrated that while the compound was effective in inducing phototoxicity in targetedcells, it also exhibited minimal dark toxicity, highlighting the importance of structuralmodifications to improve safety profiles .

5. Applications of porphyrins:

5.1. Photodynamic Therapy (PDT) for Cancer Treatment:

Mechanism: This approach relies on activating porphyrins inside the body using light of aspecific wavelength, which leads to the generation of reactive oxygen species (ROS) thatselectively destroy cancer cells.

Porphyrins Used: Compounds such as hematoporphyrin and its derivatives.

Clinical Applications: PDT is used to treat cancers of the skin, bladder, and lungs whilepreserving surrounding healthy tissues.

5.2 Bioimaging and Diagnostics:

Advantage: Porphyrins exhibit natural fluorescence, which can be exploited in bioimagingto detect tumors or sites of inflammation

Supporting Technologies: Magnetic Resonance Imaging (MRI) becomes more effectivewhen porphyrins are combined with magnetic metals.

5.3. Antimicrobial Photodynamic Therapy (aPDT):

Efficacy: This method is effective in eliminating bacteria, viruses, and fungi, includingstrains resistant to traditional antibiotics.

Principle: Upon light activation, porphyrins produce ROS that rapidly kill microbial cells.

5.4. Treatment of Dermatological Diseases:

Targeted Conditions: Psoriasis, acne, and warts.

Mechanism: Porphyrins enable the selective targeting of diseased or infected skin cellswithout damaging healthy surrounding tissues.

5.5. Nanotechnology Applications:

Integration with Nanotechnology: Porphyrins can be incorporated into nanocapsules ornanoparticles to enhance targeted delivery and achieve controlled drug release.

Outcomes: This leads to improved therapeutic efficiency, reduced toxicity, and moreprecise treatment effects.

6. Therapeutic Role of Porphyrins:

Targeted drug delivery remains a significant challenge in modern medicine. Conventionaldrugs and their delivery systems often face multiple limitations, such as poor biodistribution،inefficient clearance from the body, and uncontrolled release that does not align with thedesired pharmacodynamics. As a result, recent research has increasingly focused

on thedevelopment of smart, site-specific drug delivery systems. Within this context, porphyrinshave emerged as promising agents in therapeutic and diagnostic applications.

Porphyrins are particularly attractive due to their preferential accumulation in tumortissues, their ability to generate reactive singlet oxygen, and their low dark toxicity, makingthem especially useful in photodynamic therapy (PDT) for cancer treatment. However, oneof the major obstacles limiting their clinical utility is their poor water solubility, which adversely affects their biodistribution. To overcome this, research has shifted toward the development ofofporphyrin-based nanocomposites, aiming to enhance solubility, bioavailability, and overalltherapeutic efficacy.

Structurally, porphyrins possess a highly modifiable framework composed of four pyrroleunits linked via methine bridges. The presence of N–H groups facilitates hydrogen bondingwith anionic species, while the nitrogen atoms within the core allow for selective metal ionchelation. These properties also enable the conjugation of porphyrins to a wide range ofcarriers, including polymers and liposomes . Such structural versatility has made porphyrinsan ideal platform for chemical modification and biomedical application.

Consequently, research has increasingly focused on the post-functionalization ofporphyrins to optimize their physicochemical and biological properties, includingbiodistribution, aggregation behavior, stability, and toxicity. These functionalization strategies can be categorized into two main approaches : core functionalization—where chemical groups are introduced directly at the β- and/or meso-positions of the porphyrin ring—and peripheral are introduced directly at the β- and/or meso-positions of the porphyrin ring—and peripheral functionalization, involving modification of the substituents at the molecular periphery.

Despite the wide variety of chemical modifications explored, literature has predominantlyfocused on porphyrins incorporating metal centers, halogens, or alkynes.

Chapter 2

DIABETES

2. Diabetes

1. Definition:

Diabetes is a serious chronic disease that arises when the pancreas fails to produce sufficient insulin—a hormone that regulates blood glucose—or when the body cannot effectively use the insulin it produces. Over time, uncontrolled diabetes can lead to hyperglycemia, which may result in severe complications affecting the heart, blood vessels, eyes, kidneys, and nerves. It is estimated that over 400 million people worldwide are affected by diabetes(34).

Diabetes is classified as a metabolic disorder with multiple causes, characterized by persistent hyperglycemia and disturbances in carbohydrate, fat, and protein metabolism. These disruptions are due to inadequate insulin secretion and/or impaired insulin action(35).

2.Classification of Diabetes:

Diabetes mellitus is generally divided into four main categories: type 1 diabetes, type 2 diabetes, gestational diabetes, and other specific types, often referred to as secondary diabetes (36).

2.1. Type 1 Diabetes (Previously known as insulin-dependent diabetes):

Type 1 diabetes accounts for approximately 10% of all diabetes cases and is most commonly diagnosed in children and young adults. It results from an autoimmune destruction of the pancreatic beta cells (Langerhans islets), leading to insulin deficiency. Hyperglycemia typically manifests when only 10–20% of the insulin-producing cells remain functional (37).

2.2 Type 2 Diabetes (Previously known as non-insulin-dependent diabetes or NIDDM):

This is the most prevalent form of diabetes, representing about 90% of all diagnosed cases. It usually occurs in adults and is marked by insulin resistance and a decreased response of target tissues to insulin. Type 2 diabetes is the result of a combination of genetic predisposition and environmental factors such as excessive intake of saturated fats and sugars,

obesity, and physical inactivity. Major risk factors include family history of diabetes and belonging to a high-risk ethnic group(38).

2.3. Gestational Diabetes:

Gestational diabetes typically appears during pregnancy and is often temporary, usually resolving a few weeks after childbirth. However, women who experience gestational diabetes are at a higher risk of developing type 2 diabetes later in life (39).

2.4. Other Specific Types of Diabetes (Secondary Diabetes):

Secondary diabetes refers to diabetes that results from specific underlying conditions. According to the American Diabetes Association (ADA, 1997) and the World Health Organization (WHO, 1999), this form can be caused by pancreatic diseases, hormonal disorders, the use of certain medications or toxic substances, genetic defects that affect insulin production or action, as well as some hereditary syndromes occasionally associated with diabetes(40).

3. Symptoms of Diabetes:

Diabetes is a heterogeneous condition, meaning its symptoms and progression can vary significantly, especially between type 1 and type 2 diabetes. In some cases, it may not be possible to clearly distinguish between the two types at the time of diagnosis (41).

In particular, early symptoms—especially of type 2 diabetes—can be mild or even go unnoticed. It's possible for someone to live with diabetes for months or years without being aware of it (41).

Table1.symptoms of type 1 and type 2 diabetes (42)

Symptoms of Diabetes	
Diabetes type1	Diabetes type2
Excessive thirst and dry mouth	Excessive thirst and dry mouth

Abundant urination	Abundant and frequent Urination
Lack of energy, fatigue	Lack of energy,extreme Fatigue
Continued faith	Tingling or numbness of the hands and feet
Slow healing of wounds	Recurrent cutaneous fungal Infection
Nocturnal enuresis	Slow healing of wounds
Vision impairment	Vision impairment

4. Complications of Diabetes:

Both major types of diabetes can lead to a range of complications that may affect various organs and significantly increase the risk of early mortality. Among the serious outcomes are heart attacks, strokes, peripheral neuropathy, limb amputations, vision loss, and nerve damage.

These complications are generally categorized into:

4.1. Acute Complications:

Acute complications can occur due to sudden and extreme fluctuations in blood glucose levels. These may present as general discomfort that could progress to coma. This includes cases of severe hyperglycemia (excessively high blood sugar) or hypoglycemia (excessively low blood sugar due to treatment) (41).

4.2 Chronic Complications:

Chronic complications are generally divided into two categories:
• Macrovascular complications, such as coronary artery disease, peripheral artery disease, and strokes.
• Microvascular complications, which include diabetic encephalopathy, neuropathy, and retinopathy.
These complications arise due to damage to the small blood vessels, leading to structural and functional changes in the extracellular matrix. Such changes involve the excessive production of matrix proteins and degradation of the basement membrane, both of which are key features of diabetic microangiopathy (43).

5. Pathophysiology:

5.1. Pathophysiology of Type 1 Diabetes:

Type 1 diabetes results from the autoimmune destruction of beta (ß) cells in the pancreas. T lymphocytes produce antibodies targeting antigens on the surface of these ß cells. The immune response, along with the direct cytotoxic effect of T-killer cells, leads to the progressive destruction of the insulin-producing cells.**(44)**

5.2. Pathophysiology of Type 2 Diabetes:

In type 2 diabetes, the body becomes resistant to insulin. Although insulin is still produced, the body's cells fail to respond to it properly. Over time, the pancreas loses its ability to produce adequate amounts of insulin. This progressive dysfunction means that treatment often requires an increasing combination of medications to effectively manage the condition (45).

6. Factors Influencing Type 1 Diabetes:

a.Environmental Factors:

Studies suggest that limited exposure to infectious agents during infancy can impair the proper development of the immune system. This under-stimulation may increase the likelihood of autoimmune diseases such as type 1 diabetes

b.Genetic Factors

Type 1 diabetes is associated with more than 20 different regions of the human genome. Among the most significant are the HLA (human leukocyte antigen) region on chromosome 6p21, and the insulin gene region on chromosome 11p15—previously referred to as DSID2 or IDDM2 in English. The specific HLA types linked to the disease vary depending on the population studied (46).

c.Immunological Factors:

Type 1 diabetes is a chronic autoimmune disorder primarily driven by T lymphocytes. Family studies have shown that the immune system gradually destroys pancreatic beta cells over several years through the production of autoantibodies targeting the pancreas (47). Symptoms such as hyperglycemia typically do not appear until around 80% of beta cells have been destroyed (48). This type of diabetes is often associated with other autoimmune diseases, including thyroid disorders, celiac disease, and certain types of anemia (49).

d.Viral Infections:

Several viruses have been linked to the onset of type 1 diabetes, including retroviruses, cytomegalovirus, Epstein-Barr virus, coxsackievirus, and rubella virus. These viruses may contribute to the disease by directly infecting and destroying beta cells, or indirectly by exposing autoantigens, activating self-reactive lymphocytes, or mimicking autoantigen structures that trigger an immune response (50).

7. Factors Influencing Type 2 Diabetes:

a. Genetic Factors:

Family-based studies have confirmed the strong genetic contribution to the development of type 2 diabetes. In monozygotic twins, the concordance rate ranges from 60% to 100%,

indicating a significant hereditary component. Among individuals with early-onset type 2 diabetes, the likelihood of familial occurrence is around 40% (51).

b. Environmental Factors:

Environmental and lifestyle factors play a key role in the onset of type 2 diabetes. Advancing age, physical inactivity, smoking, obesity—particularly central or abdominal obesity—and a sedentary lifestyle all significantly elevate the risk of developing the disease(52).

Insulin Secretion Abnormalities:

Insulin secretion by the beta cells in the pancreatic islets of Langerhans follows a biphasic pattern in response to increased glucose levels:

1. First phase: A rapid and sharp release of insulin occurs within minutes of a rise in extracellular glucose concentration—this is the early peak.
2. Second phase: If the glucose levels remain elevated, a slower and sustained release of insulin follows—this is the late phase.

This biphasic secretion is crucial for maintaining normal blood glucose levels, and its disruption is a hallmark of type 2 diabetes (53)

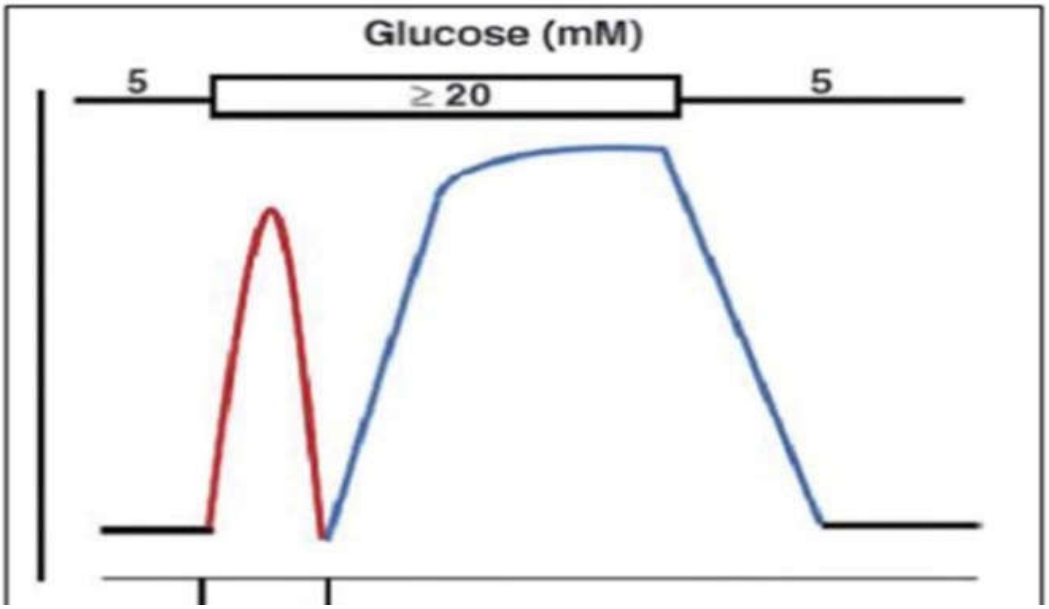

Figure5.Biphasic secretionof insulin in responseto a constant glucose**.**

Insulin Sensitivity Disorders:

Fasting hyperglycemia and some post-meal (postprandial) hyperglycemia can be attributed to excessive glucose production by the liver, which results from reduced insulin effectiveness on insulin-sensitive tissues such as muscles, adipose tissue, and the liver itself (54).

This condition, known as insulin resistance, is particularly evident in impaired glucose uptake by muscles and fat tissues, as well as increased glucose synthesis by the liver. Moreover, elevated levels of circulating free fatty acids and triglycerides accumulated in muscle tissue further aggravate insulin resistance. High concentrations of these fatty acids also stimulate increased glucose production by the liver (55).

8.Treatments :

8.1. Medical Treatments:

- Oral hypoglycemic agents:

Oral antidiabetic drugs are able to normalize blood glucose levels in fewer than half of treated patients. However, they do not reverse already established diabetic complications and are contraindicated in cases of liver or kidney failure. Additionally, their side effects should not be overlooked.

When a single therapy fails to control type 2 diabetes, healthcare providers may choose from five different classes of oral hypoglycemic agents, each working through various mechanisms:

• **Sulfonylureas (e.g., Glibenclamide):** Stimulate insulin secretion from pancreatic beta cells,without affecting insulin synthesis.

• **Biguanides (e.g., Metformin):** Improve insulin sensitivity by enhancing its action on target tissues, inhibiting hepatic gluconeogenesis, and reducing glucose absorption in the intestine—without influencing insulin secretion.

• **Alpha-glucosidase inhibitors (e.g., Acarbose, Miglitol):** Slow the digestion and absorption of complex carbohydrates in the intestine.

• **Thiazolidinediones (Glitazones):** Increase insulin sensitivity and improve the function of pancreatic beta cells.

• **Glinides:** Act as insulin secretagogues, promoting insulin release.

a. Insulin Administration:

When oral therapy is no longer effective in managing type 2 diabetes, insulin treatment should be initiated as early as possible to preserve the remaining insulin sensitivity. Insulin therapy often leads to significant improvements in glycemic control.

Additionally, insulin becomes essential in patients for whom oral antidiabetic drugs are contraindicated (such as those with kidney or liver failure).

Insulin preparations vary based on their onset of action, peak activity, and duration. Therefore, insulin therapy should be tailored to the individual based on therapeutic goals, age, general health, dietary habits, physical activity, awareness of hypoglycemia, and ability to self-manage treatment.

Despite the wide array of available treatments and lifestyle measures, achieving optimal blood glucose control remains a major challenge in diabetic care (37).

8.2. Phytotherapy:

Phytotherapy, or the use of plants for therapeutic purposes, has long been employed across many areas of medicine. Its popularity stems from several advantages: minimal side effects, absence of synthetic chemicals, and affordability.

- Diabetes has been managed traditionally through Chinese medicine, folk remedies, and more systematically through phytotherapy. Numerous in vitro and in vivo studies have demonstrated that certain plants possess active hypoglycemic compounds such as polyphenols, alkaloids, saponins, coumarins, and terpenoids.

However, there is currently no evidence-based recommendation for the use of phytotherapy, either alone or in combination with conventional treatments, in managing hyperglycemia and its complications (56).

In Algeria, several plants with hypoglycemic properties are traditionally used, including:

• El Bane (Moringa oleifera)
• Mor et Sbor (Aloe vera L.)
• Chih (Artemisia herba-alba Asso)
• Louben (Boswellia sacra Flueck)
• Tai Lakhdar (Camellia sinensis)
• El Halba (Trigonella foenum-graecum L.) (57)

8.3. Mechanisms of Action of Medicinal Plants:

Pharmacological research has identified several mechanisms through which medicinal plants exert antidiabetic effects. Because these plants contain various chemical compounds, they may act on multiple pathways to reduce blood glucose levels (Jarald et al., 2008; Kashikar & Kotkar, 2011; Singh et al., 2012). These mechanisms include:

• Stimulating insulin secretion from pancreatic β-cells and/or promoting their regeneration or reducing insulin resistance.

• Enhancing β-cell activity by providing essential elements such as copper (Cu++), magnesium (Mg++), and calcium (Ca++), or through revitalization and/or hyperplasia of these cells.

• Reducing glucagon secretion, which in turn decreases glucose absorption in the intestines and increases peripheral glucose uptake.

• Modulating liver enzyme activity to promote glycogenesis (glucose storage) and/or inhibit glycogenolysis (glucose breakdown).

• Inhibiting digestive enzymes like α-amylase and α-glucosidase, thereby slowing carbohydrate breakdown and reducing glucose absorption in the intestines.

• Affecting renal glucose reabsorption in the proximal tubules, as seen with substances like phloridzin (58).

• Enhancing glucose uptake by adipose and muscle tissues or blocking intestinal glucose transporters to limit glucose entry into the bloodstream.).

9.Blood glucose regulation:

9.1 The Role of Insulin:

Insulin is widely recognized as the primary pancreatic hormone responsible for the precise regulation of blood glucose levels. It facilitates the storage of fats in adipose tissue and promotes the conversion of glucose into glycogen in the liver and muscles. Notably, insulin is the only hormone with hypoglycemic properties, and it is secreted by the β-cells of the islets of Langerhans in the pancreas..

9.2. Glucose as a Stimulator of Insulin Secretion:

The GLUT2 transporter, a non-insulin-dependent glucose transporter, is found on the surface of pancreatic β-cells. This transporter allows glucose to pass freely from the bloodstream into the β-cell. Once inside the cell, glucose is directly sensed by the pancreas, initiating a series of metabolic events that result in insulin secretion.

The initial step involves an increase in the ATP/ADP ratio as the glucose is metabolized. Elevated levels of ATP lead to the closure of ATP-sensitive potassium (K^+) channels by binding to the Kir6.2 protein subunit (59). This closure causes membrane depolarization of the β-cell, which then triggers the opening of voltage-dependent calcium (Ca^{2+}) channels (60).

The resulting rise in intracellular calcium concentration leads to the exocytosis of insulin-containing vesicles, a process mediated by the SNARE protein complex (Henquin J-C, 2000). This entire sequence allows the pancreas to effectively release insulin in response to increased blood glucose levels.

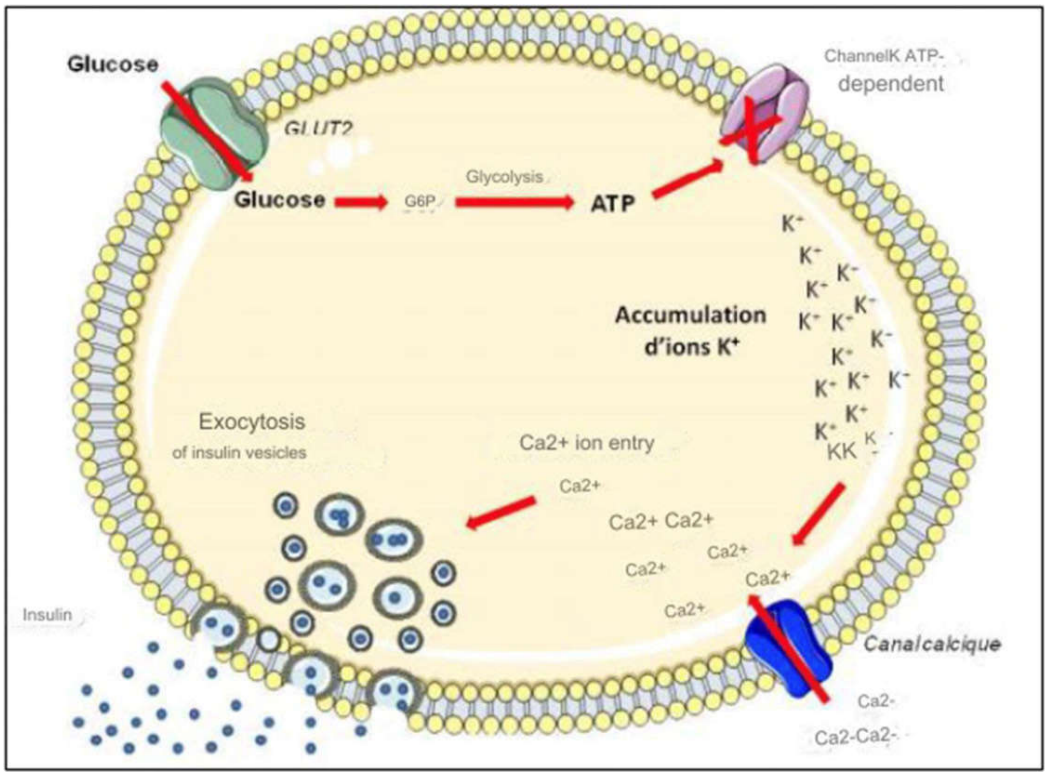

Figure14.secretion of insulin by the pancreatic β-cells(61)

9.3. Insulin Signaling Pathways:

Once insulin enters the systemic circulation and binds to its specific receptor on the surface of target cells—primarily muscle, adipose, and liver tissues—it triggers a cascade of anabolic responses. This insulin receptor possesses intrinsic tyrosine kinase activity, which allows it to phosphorylate specific tyrosine residues on intracellular substrates, primarily the Insulin Receptor Substrates (IRS) and SHC (Src Homology and Collagen) adaptor proteins (62).

Two major intracellular signaling pathways are activated:

1. The PI3K (Phosphatidylinositol 3-Kinase) Pathway:Responsible for insulin's metabolic effects, such as glucose uptake and glycogen synthesis.

2. The MAPK (Mitogen-Activated Protein Kinase) Pathway:Involved in cell growth, proliferation, and differentiation.

The proteins IRS1 and IRS2 play a key role in transmitting insulin's signal inside the cell (63). Through this signaling cascade, insulin facilitates the translocation of the GLUT4 transporter to the surface of muscle and fat cells, enhancing glucose uptake (64). In the liver, insulin directly activates proteins and transcription factors involved in regulating glucose metabolism.

9.4. Glucagon Signaling Pathways:

The glucagon receptor is a 63 kDa membrane glycoprotein (Iyengar R. et al., 1984) and a member of the G protein-coupled receptor (GPCR) family with seven transmembrane domains. It is widely expressed in several tissues, including the liver, heart, intestines, brain, adipose tissue, and pancreas (65).

Upon glucagon binding, the receptor activates small G proteins, primarily Gs and Gq (66):

• Gs Protein Coupling:

Activates adenylate cyclase, increasing cyclic AMP (cAMP) levels. This leads to Protein Kinase A (PKA) activation, which stimulates glycogenolysis and activates PGC-1α, a transcription factor that promotes genes involved in glucose production.

• Gq Protein Coupling:

Activates phospholipase C (PLC), leading to an increase in intracellular calcium levels. This calcium rise further supports the action of PGC-1α, contributing to the upregulation of metabolic gene expression (61).

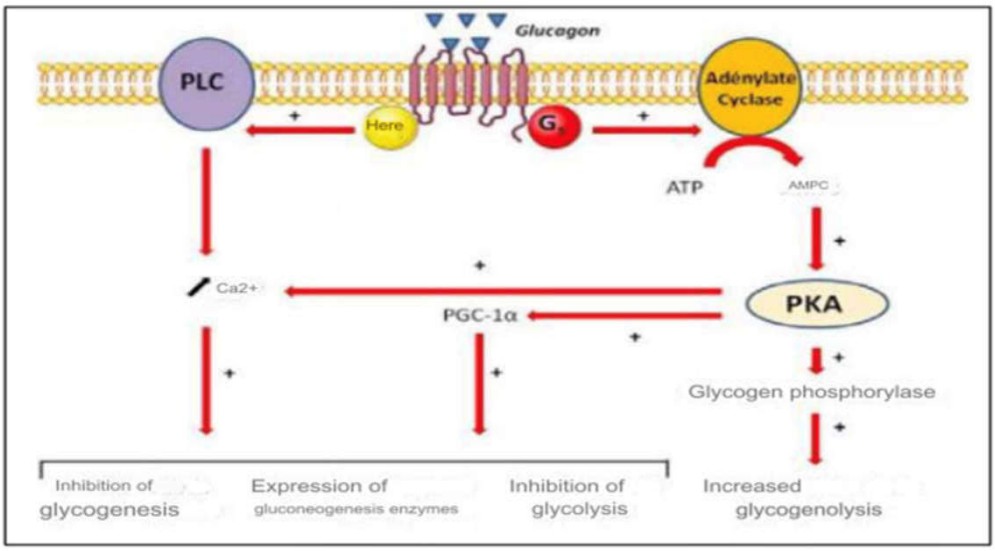

Figure 15. Glucagon signaling pathway

10. The Enzymatic Regulation of Glucose Metabolism:

10.1. Alpha-Amylase:

Definition:

Alpha-amylase is a globular protein enzyme, typically classified as a macromolecule. It is found ubiquitously in living organisms. This endo-enzyme, with a molecular mass ranging between 40 and 70 kDa, catalyzes the random hydrolysis of α-1,4-glycosidic bonds in polysaccharides such as glycogen, amylose, and amylopectin, while leaving the terminal bonds intact. The hydrolysis process produces glucose and maltose as the primary products.

a. Nomenclature:

• Common Name: Alpha-amylase

• Other Names: Glycogenase, alpha-amylase, endoamylase, Taka-amylase A, maxilase

• Systematic Name: 1,4 alpha-D-glucan-4-glucano hydrolase (67)

b. Types of Amylase:

There are several types of amylase, including alpha (EC 3.2.1.1), beta (EC 3.2.1.2), and gamma (EC 3.2.1.3) amylases. Beta- and gamma-amylases (also known as glucoamylases) are generally found in plants and microorganisms, although certain mammals and aquatic species may also possess glucoamylase. A critical feature of these enzymes is the production of α-dextrins .

c. Synthesis Location:

In humans, amylase is primarily secreted by the salivary glands (salivary amylase, also known as amylase S) and the pancreas (pancreatic amylase, or amylase P). The human amylases are encoded by two genes, Amy1 and Amy2A, located on chromosome 1 (68).

Amylase S consists of two protein families:

• Family A proteins: These are glycosylated and have a molecular weight of 62 kDa.

• Family B proteins: These are non-glycosylated and have a molecular weight of 55 kDa.

d. Structure:

Human pancreatic alpha-amylase (HPA) is a monomeric protein that requires calcium and chloride ions for optimal activity. Although the amino acid sequence and structure of salivary alpha-amylase and pancreatic alpha-amylase are similar, they are generally not discussed separately. The HPA enzyme consists of three structural domains.

• Domain A (orange and red): The largest domain, containing an eight-stranded β/α-barrel structure, which houses the active site (Asp197, Glu233, Asp300) and a chloride-binding site (Arg195, Asn298, Arg337). It spans residues 1-99 and 169-404.

•Domain B (sky blue; residues 100–168) is the smallest of the three domains. It is located on an extended loop between the third β-strand and the α-helix of the β-barrel core of Domain A. This domain contains a calcium-binding site composed of residues Asn100, Arg158, and Asp167, along with His201 from Domain A.

Domain C (pink; residues 405–496) is located at the C-terminal end of the protein. Its exact function remains unclear. It is characterized by an anti-parallel β-sheet structure and is connected to Domain A (69).

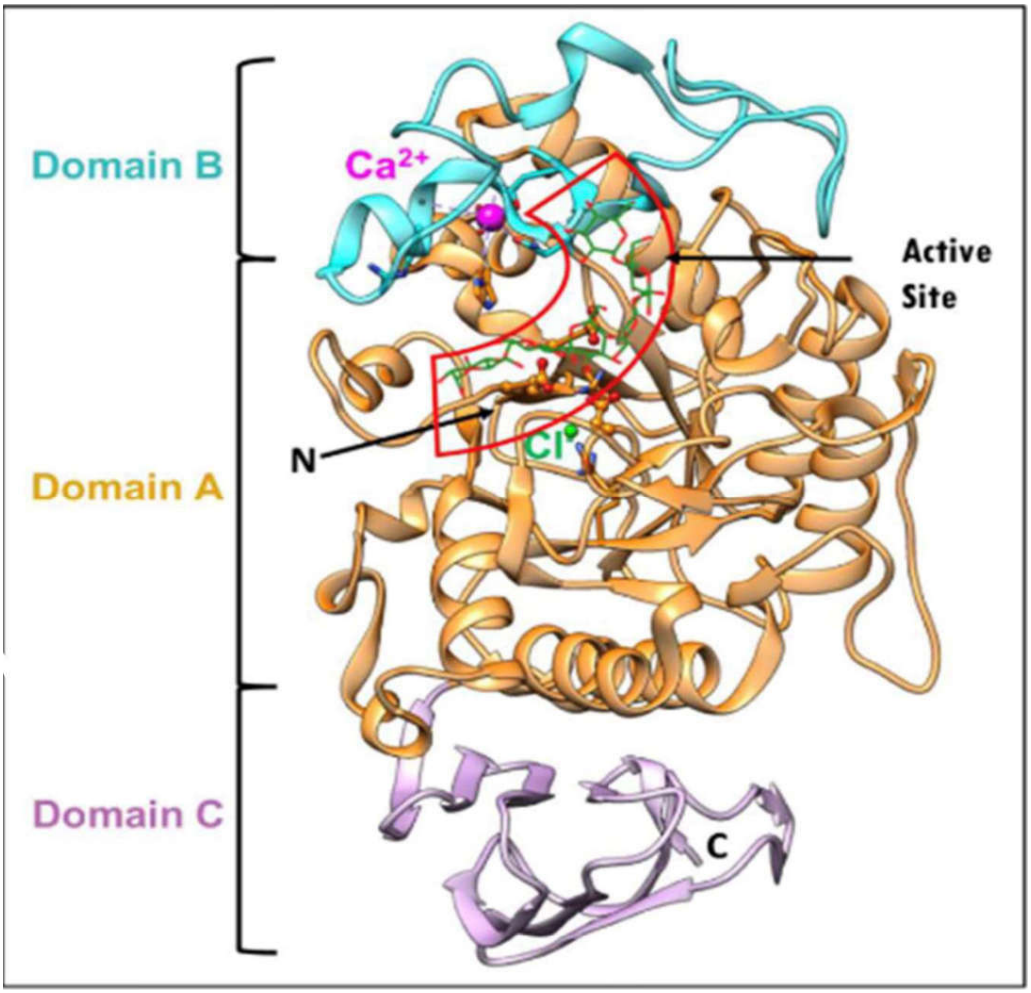

Figure16. Ribbon diagram of human pancreatic alpha-amylase(HPA)and its subdomains in complex with an octaose substrate (69).

e.Physical and Chemical Properties of Alpha-Amylase:

Molecular Weight:

The molecular weight of alpha-amylase varies depending on the species and origin, typically ranging between 40,000 and 90,000 Daltons (67). In legumes, alpha-amylases generally range from 40,000 to 70,000 Daltons .

Optimal Temperature:

The optimal temperature for alpha-amylase activity depends on its origin and ranges from 40°C to 90°C (67). Bacterial alpha-amylase, particularly from Bacillus amyloliquefaciens, exhibits high thermostability and can operate effectively at 70°C to 90°C. In contrast, fungal alpha-amylases typically function best between 50°C and 70°C.

Optimal pH:

Alpha-amylase is highly sensitive to pH, making pH optimization essential for its activity. According to Kindle (1983), alpha-amylase exhibits optimal activity within a pH range of 4 to 8. Bacterial alpha-amylases tend to have an optimal pH above neutral, while fungal alpha-amylases function best between pH 4 and 6 (Larpent et al., 1992). For yeast-derived enzymes, the effective pH range is also between 4 and 6 .

Effectors:

Effectors, which include activators and inhibitors, influence enzyme activity by interacting directly or indirectly with the enzyme's active site (Garrett & Grisham, 2000). Inhibitors are typically structural analogs of the substrate that either do not react or react very slowly. Studying inhibitors helps in understanding the enzyme's catalytic mechanism, specificity, and the structural characteristics of its active site.

Ions such as Cu^{2+}, Fe^{2+}, and Hg^{2+} act as competitive inhibitors and structural analogs (Mercier, 1985). Conversely, Ca^{2+} and Mg^{2+} act as activators, contributing to the stability and function of alpha-amylase. However, excessive calcium concentrations (above 20 mM) can have an inhibitory effect.

Substrate Specificity:

Starch (amidon) is the natural substrate for alpha-amylase. It consists of glucose units linked by α(1→4) glycosidic bonds forming helical chains (amylose), and occasionally branched by α(1→6) bonds (amylopectin). The production of alpha-amylase in fungal species such as Aspergillus, Rhizopus, and Penicillium is regulated by the presence of starch, which

induces enzyme synthesis. Salivary alpha-amylase initiates starch digestion in the mouth and continues this process in the small intestine.

f. Function of Alpha-Amylase:

The breakdown of starch, the primary dietary source of glucose in humans, begins in the mouth. Saliva contains alpha-amylase, which hydrolyzes internal α(1→4) glycosidic bonds in starch molecules—except for those at the terminal ends and near branch points. As food is chewed and mixed with saliva, alpha-amylase begins breaking down long starch chains. By the time the food reaches the stomach and the enzyme is inactivated by gastric acidity, the average length of the starch chains is reduced from several million glucose units to fewer than 800.

In the small intestine, starch digestion resumes with the action of pancreatic alpha-amylase, which is functionally similar to salivary alpha-amylase, and β-amylase, which acts from the non-reducing ends of the chains. This digestion process yields a mixture of maltose (a disaccharide), maltotriose (a trisaccharide with three glucose units linked by α(1→4) bonds), and dextrins (oligosaccharides that contain α(1→6) branch points).

These oligosaccharides are further hydrolyzed by specific enzymes located on the brush-border membranes of the intestinal mucosa. Among these enzymes is α(1→6) glucosidase, which cleaves glucose residues one by one from branched oligosaccharides, ultimately converting them into absorbable monosaccharides (70).

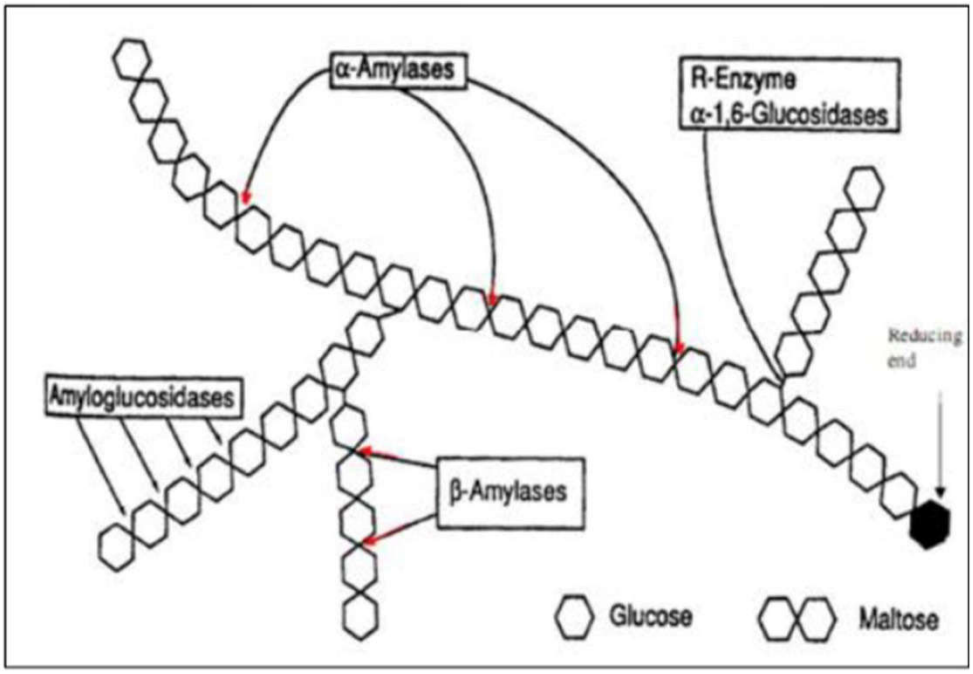

Figure6. EnzymaticDigestion of starch(71)

Mechanism of Action of Alpha-Amylase:

The catalytic activity of alpha-amylase involves three key amino acid residues at the active site: Aspartic acid 231 (the catalytic nucleophile), Glutamic acid 261 (acts as a proton donor), and Aspartic acid 328 (plays a supporting catalytic role).

The enzyme's activity is highly dependent on temperature and pH. pH influences the ionization state of the amino acids at the catalytic site, affecting their ability to participate in proton transfer, which is essential for breaking glycosidic bonds. Temperature, on the other hand, facilitates the formation of the enzyme-substrate complex by increasing molecular motion (72).

Although the full catalytic mechanism is not yet completely understood, it is believed to follow a probabilistic multi-step process involving the following four phases:

1. Formation of the Enzyme-Substrate Complex:

The enzyme binds to the starch chain either at internal regions or at the reducing ends. The substrate undergoes conformational changes upon binding, which are stabilized by

multiple hydrogen bonds between the polar hydroxyl groups of the carbohydrate chain and amino acid residues at the enzyme's binding site (72).

2. Cleavage of the α(1→4) Glycosidic Bond:

At the catalytic site, the protonated glutamic acid donates a proton to the oxygen of the glycosidic bond, weakening it and facilitating its cleavage from the C4 position. Simultaneously, the ionized aspartic acid forms a covalent bond with the anomeric carbon (C1), releasing the first segment of the sugar chain (73).

3. Restoration of the Enzyme:

A water molecule hydrolyzes the bond between C1 and the aspartic acid. The negatively charged glutamic acid abstracts a proton from the water molecule, while the remaining hydroxyl group attaches to the anomeric carbon (C1), breaking the covalent linkage with aspartic acid.

4. Release of the Second Product Segment:

Following the hydrolysis step, the second part of the cleaved carbohydrate chain is released, and the enzyme is regenerated to its original form (73)

In this mechanism, glutamic acid functions as a general acid catalyst and proton donor, while aspartic acid acts as a nucleophile or general base catalyst, facilitating the cleavage of the glycosidic bond in a typical nucleophilic substitution reaction (73).

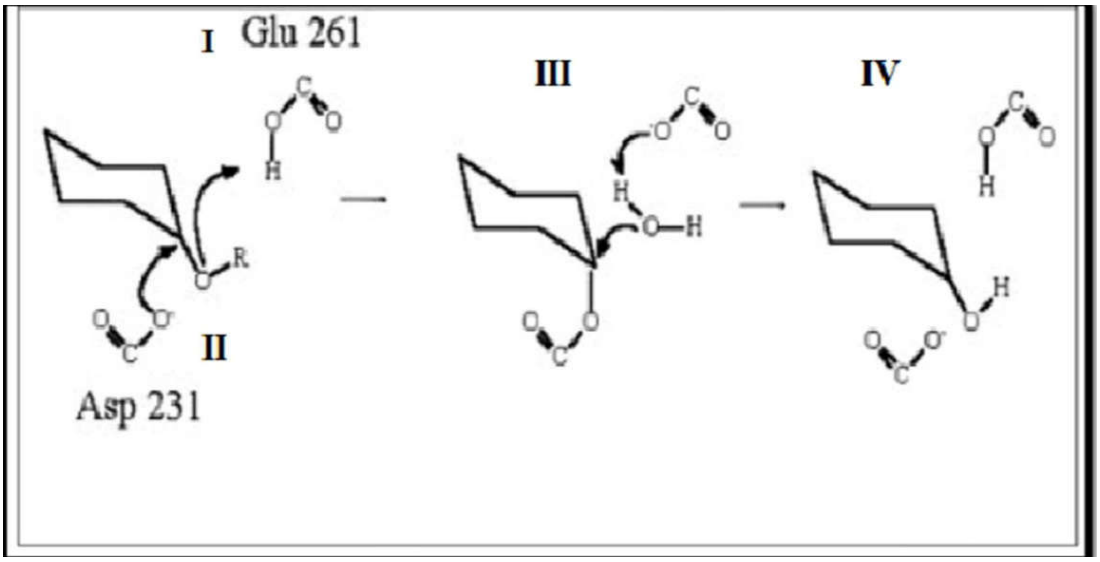

Figure18. Catalytic machanism of glycosyl hydrolases

10.2. Alpha-Glucosidase:

According to IUPAC-IUBMB nomenclature, alpha-glucosidases (EC 3.2.1.20; α-D-glucoside glucohydrolase) are a group of exo-glycosidase enzymes that specifically catalyze the hydrolysis of α-1,4-glycosidic bonds found in substrates such as glycogen and malto-oligosaccharides, leading to the release of α-D-glucose. In addition to their hydrolytic activity, alpha-glucosidases are also capable of performing transglycosylation reactions, resulting in the formation of α-D-glucosylated compounds

11. Acarbose:

Mechanism of Action:

Acarbose is a pseudotetrasaccharide derived from microbial sources. It functions at the intestinal brush border by competitively inhibiting alpha-glucosidase enzymes, thus slowing down the enzymatic breakdown of complex carbohydrates such as disaccharides, oligosaccharides, and polysaccharides into absorbable monosaccharides. This inhibition leads to a reduction in postprandial hyperglycemia without causing hyperinsulinemia or changes in body weight (74)

SECOND PART

EXPERIMENTAL

Chapter one: Materials and methods

1. chemicals and reagents

1.1Alpha Amylase:

A solution of alpha-amylase (commercially marketed as Megamylase with a specific activity of 3000 (U. CEIP/cp) at a concentration of 0.5 mg/ml) was prepared in a phosphate saline buffer (pH = 6.4).

1.2.Acarbose:

Different concentrations of acarbose solution (commercially marketed as Acorbay 50 mg) were prepared in a phosphate saline buffer (pH = 6.4).

1.3.Substrate:

As a substrate, soluble starch was utilized. 250 mg of starch was dissolved in 25 ml of distilled water at a temperature of 50 to 70°C under agitation.

1.4.Lugol:

The Lugol solution (KI/I2; Sigma-Aldrich Chemical) was obtained commercially from Sigma-Aldrich and utilized as a staining reagent in the study. Stored at room temperature in a dark container.

1.5.Phosphate Buffer Solution:

The phosphate buffer saline solution was meticulously prepared using sodium dihydrogen phosphate and disodium hydrogen phosphate (Sigma Aldrich) in conjunction with double distilled water and KCl. The pH was meticulously maintained at 6.4 through the utilization of this phosphate buffer.

2. In Vitro alpha-amylase inhibition assay

Inhibition of α-amylase activity was carried out as described by E. Deveci et al (Deveci et al., 2020), with nuanced adjustments. Briefly, A starch solution (1% w/v) was

prepared by stirring 1g starch in 100 ml of 20 mM of phosphate buffer (pH 6.9) containing 6.7mM of sodium chloride. The enzyme solution was prepared by mixing 50 mg of α-amylase in 100 ml of 20 mM of phosphate buffer (pH 6.9 with potassium chloride) to 200 µl of appropriate dilutions (1 - 2µg/mL) From porphyrin ,500 µl of alpha amylase solution was added and the mixture was incubated at 37 ºc for 10 min. To the reaction mixture 100 µl (1%) starch solution was added and incubated at 37ºC for 10 min. The reaction was stopped by addition of 25 µL HCl (0.1 M) and 100 µL Lugol solutions and kept it in a boiling water bath for 5 minutes and cooled to room temperature. The reaction mixture was then diluted to 2 ml with distilled water, and absorbance measured at 545 nm with UV–Vis spectrometer, (Shimadzu 1800, Japan) using a cell of 1 ml with an optical path length of 1 mm. For each concentration, blank tubes were prepared by replacing the enzyme solution with 500 µL in distilled water. The experiment was repeated using acarbose as a standard antidiabetic drug (positive control). The experiments were repeated thrice using the same protocol. The alpha-amylase inhibitory activity was expressed as percentage inhibition. The percentage inhibition was calculated using the following.

$$\% \text{ Inhibition} = \left(\frac{A - A_0}{A} \right) \times 100$$

Where, A represents the absorbance of negative control (enzyme activity in the absence of the standard inhibitor or extract). B is the absorbance of test assay (enzyme activity in the presence of only the extract or only the standard inhibitor).

3. In-Silico analysis

3.1 Materia and Methods

3.1.1Computational details:

The geometric optimization of all synthesized compounds was carried out using theGaussian 09 program package [75] . The Density Functional Theory (DFT) approach wasemployed, specifically the Becke's three-parameter hybrid exchange functional combinedwith the Lee-Yang-Parr correlation functional (B3LYP), in conjunction with the

6++311-G(d,p) basis set [76] . This functional and basis set combination was selected for itsproven ability to accurately predict molecular geometries, electronic properties, and reactivity.descriptors for a wide range of organic compounds at a reasonable computational costUpon obtaining the optimized geometries, a detailed quantum chemical analysis wasperformed to compute several global reactivity descriptors. These include the energy gap (ΔE GAP), ionization energy (I), electron affinity (A), electronegativity (χ), electronic chemicalpotential (μ), chemical hardness (η), chemical softness (S), and electrophilicity index (ω).

These parameters were calculated using the frontier molecular orbital energies—namely, the highest occupied molecular orbital (HOMO) and the lowest unoccupied molecular orbital

(LUMO):—according to conceptual DFT definitions [77] . The relevant equations are

- ✓ Energy gap: (2)
- ✓ Ionization Energy: (3)
- ✓ Electron Affinity: (4)
- ✓ Electronegativity: (5)
- ✓ Chemical Potential: (6)
- ✓ Chemical Hardness: (7)
- ✓ Chemical Softness: (8)
- ✓ Electrophilicity Index: (9)

These descriptors offer valuable information about the stability, reactivity, and electrophilicor nucleophilic nature of the studied molecules. In particular, the HOMO-LUMO energy gap(ΔE GAP) serves as an important indicator of chemical reactivity and kinetic stability:

a smallergap typically corresponds to higher chemical reactivity and lower kinetic stability. Similarly‹the electrophilicity index (ω) quantifies the molecule's ability to accept electrons, which issignificant in understanding potential interactions with biological targets.

3.2. Cheminformatics Prediction:

3.2.1.PASS Online:

The molecular structures of all synthesized compounds were initially sketched usingChemDraw® Ultra software, version 12 (CambridgeSoft Corporation, 1986–2009, Akron‹OH, USA). Following the drawing phase, each structure underwent a rigorous verificationprocess, ensuring chemical correctness by utilizing the “Clean Structure” tool. This stepoptimized bond angles and atom placements to produce chemically reasonable, low-strainconformations suitable for computational analysis. Once verified, the structures were exportedand saved in the MDL Molfile format (.mol), a standard file type that preserves detailedatomic and bonding information necessary for further in silico analyses.

The generated Mol files were then uploaded to the PASS (Prediction of Activity Spectrafor Substances) online server (http://195.178.207.233/PASS/index.html) [78] . PASS softwareemploys advanced machine learning algorithms based on Multilevel Neighborhoods of Atoms (MNA) descriptors to predict the biological activity spectra of chemical compounds. Afteruploading, the "Predict Activity" function was activated to obtain a comprehensive list ofpotential biological activities. Each predicted activity was accompanied by two values: theprobability "to be active" (Pa) and the probability "to be inactive" (Pi). Only activities with aPa value greater than 0.5 were considered statistically significant and retained for furtherinterpretation, as higher Pa values indicate a greater likelihood that the compound exhibits thepredicted biological activity in experimental settings.

3.2.2.ADMET Prediction:

For the evaluation of pharmacokinetic and drug-likeness properties, the chemical structuresof the synthesized compounds were processed using the SwissADME online server [79].

Initially, the “Import” function within the molecular sketcher interface was utilized to uploadthe previously prepared structures in MDL Molfile (.mol) format. Upon successfulimportation, each molecular structure was visually confirmed and automatically rendered inthe sketcher window. The structures were subsequently converted into the SimplifiedMolecular Input Line Entry System (SMILES) notation, a compact representation formatnecessary for computational processing.

After ensuring the accuracy of the SMILES translation, the "Run" command was executed to initiate the prediction analysis. The SwissADME server then generated a comprehensive set of pharmacokinetic parameters, including absorption, distribution, metabolism, and excretion(ADME) profiles, as well as drug-likeness evaluations based on Lipinski’s Rule of Five Ghose, Veber, Egan, and Muegge criteria. Additionally, properties such as gastrointestinal(GI) absorption, blood-brain barrier (BBB) permeability, and interactions with cytochromeP450 isoforms were predicted. These parameters are critical for assessing the drug potentialand biopharmaceutical properties of the designed compounds at an early stage of drugdiscovery.

3.3. Molecular Docking

3.3.1.Ligands Preparation:

The two-dimensional (2D) chemical structure of the reference standard, acarbose, wasretrieved from the PubChem database [80] (https://pubchem.ncbi.nlm.nih.gov/). Followingretrieval, the structure was converted into a three-dimensional (3D) conformation usingenergy minimization tools integrated within molecular modeling software to ensure ageometrically optimized and chemically accurate 3D model suitable for docking studies.

Structural optimization procedures were performed to reduce any steric clashes and to refine bond angles and torsions.

In parallel, the preparation of the porphyrin ligands was conducted according to theprotocol described in the Computational Details section. This included geometry optimization at the Density Functional Theory (DFT) level and generation of appropriate

file formats required for molecular docking simulations. Both the standard (amoxicillin) and the studied ligands were thus standardized under the same preparation conditions to ensure comparability and accuracy in subsequent docking evaluations .

3.3.2.Receptor Preparation:

For the investigation of antidiabetic potential, the human pancreatic α-amylase enzymewas selected as the biological target. The three-dimensional (3D) crystallographic structure of α-amylase (Protein Data Bank ID: 1HNY) was retrieved from the RCSB Protein Data Bankhttps://www.rcsb.org/) [81] .

Initial preparation of the receptor was performed using AutoDock Tools (ADT) [82] . The preparation protocol involved the removal of all crystallographic water molecules, ligands, and cofactors to isolate the raw protein structure suitable for docking studies. Thereafter, polar hydrogen atoms were added to the receptor to correctly modelhydrogen bonding interactions, and Kollman partial atomic charges were assigned to facilitate accurate electrostatic calculations. Furthermore, the active site was carefully defined based on the co-crystallized ligand position and known catalytic residues, ensuring precise docking grid setup for subsequent molecular docking simulations.

3.4. Molecular Docking Studies:

To evaluate the binding affinities between the human pancreatic α-amylase receptor andthe studied ligands, an automated molecular docking procedure was carried out usingAutoDock 4 software [83] . The binding site of the receptor was defined by generating a gridmap with AutoGrid, centering it around the known active site of α-amylase. The griddimensions were set to 80 × 80 × 80 points with a spacing of 0.5 Å between grid points, andcentered at coordinates X=62.85, Y=49.85, and Z=18.34.

Ligand preparation involved the definition of all rotatable bonds using the autotors utilityembedded within AutoDock Tools, enabling flexible ligand docking while treating the receptoras rigid. Docking simulations were conducted employing the Lamarckian

Genetic Algorithm (LGA) with the following parameters: 10 docking runs per ligand, a population size of 150individuals, a maximum of 250,000 energy evaluations, a maximum of 27,000 generations, amutation rate of 0.02, a crossover rate of 0.8, and an elitism value of 1, while other settingswere maintained at default values.

Post-docking, the pose corresponding to the lowest binding free energy (expressed inkcal/mol) was selected as the most favorable binding conformation for each ligand. Theselected docking poses were subjected to further interaction analysis using the Protein-Ligand Interaction Profiler (PLIP) web server [84] , enabling detailed visualization of hydrogen bonds, hydrophobic contacts, salt bridges, and π-stacking interactions between ligands and the receptor.

Chapter two: results and discussion

Results AND DISCUSSION:

1. Alpha-amylase inhibitory activities (IC50):

The in-vitro antidiabetic potential of porphyrins was investigated using α-amylase inhibition model and theresults are as shown in Table2. *From the exponential of Porphyrin* concentration (µg/mL) against percentage α-amylase inhibition (Figure.19 and.20),the studied E Porphyrins significantly increased α-amylase inhibition (%) with corresponding increasein E Porphyrins concentration. The effective inhibitory concentration (IC50 value) at which 50% of αamylase activity was inhibited by Porphyrin was obtained to be 0.366 and 0.016and11.166 and 0.004 µg/mL respectively indicating a powerful potential to slowdown starch digestion via α-amylase inhibition.

The inhibitory potential of acarbose, a standard type 2 antidiabetic drug, on α-amylaseactivity was also analysed in the present study to serve as positive control. The result obtained Porphyrins showed that the inhibited α-amylase with more degree , show a more degree, compared to acarbose (IC50=11.166 µg/mL) (Figure.20).

Metabolism of carbohydrate (complex sugar or polysaccharide) by hydrolases (such as α amylase, α-glucosidase, maltase etc.) leads to release of simple sugars such as glucose and thus boosts blood sugar level rise immediately after consumption of a carbohydrate-rich food; inhibitors of α-amylase, amongst others, are thus very useful in preventing sudden rise in blood glucose level especially in type 2 diabetic patients, following their consumption of carbohydrate-rich food substances .

The relatively inhibitory prowess of the For the studied porphyrins as α-amylaseinhibitor compared to acarbose is a desirable property in the present study. This is becauseprevious studies had reported that the extremely high inhibitory effect of acarbose against αamylase eventually leads to excessive delay of starch hydrolysis in gastrointestinal tractthereby causing abdominal discomfort and flatulence in diabetic patients who take the drug.

Porphyrin 1 curve

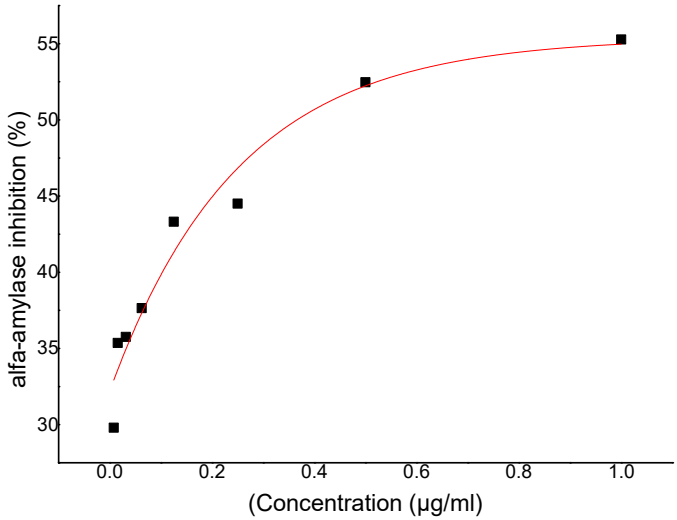

Porphyrin 2 curve

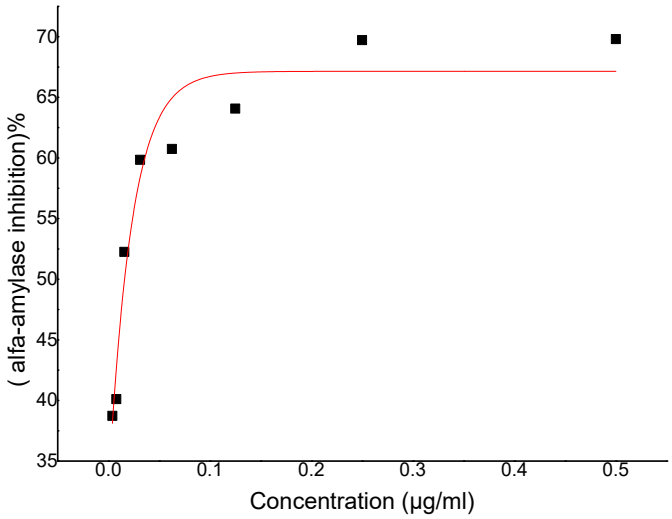

Figure19. Exponential regression of the inhibition of α-amylase activity by the Porphyrins: Porphyrin1 and Porphyrin 2**.**

Porphyrin 3 curve

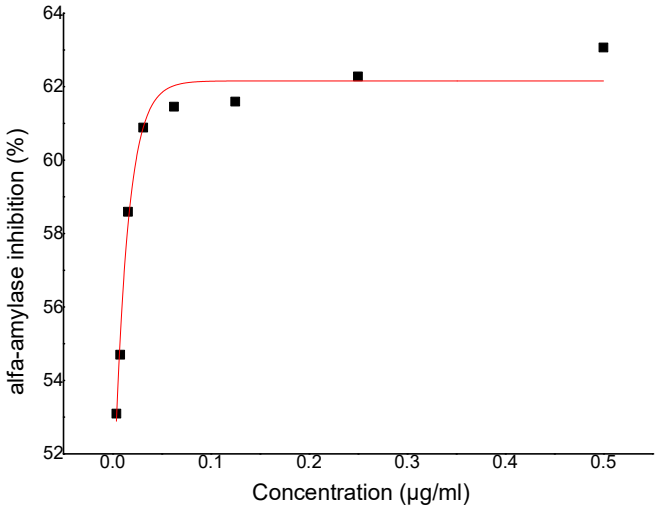

Porphyrin 4 curve

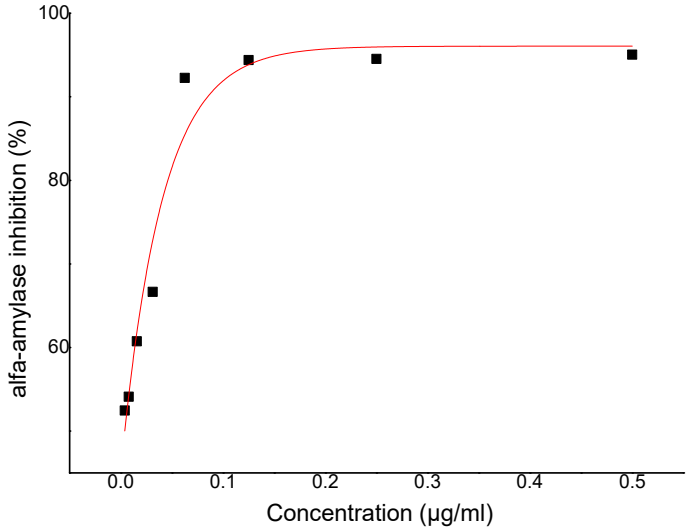

Figure20. Exponential regression of the inhibition of α-amylase activity by the Porphyrins: Porphyrin3 and Porphyrin4**.**

Table2. In vitro Anti-diabetic activity of the porphyrins by α-amylase inhibitory assay

Sampls porphyrins	Concentration (µg/mL)	Percentage of α-Amylase Inhibition	IC50 Values
P1	1	55.274	
P1	0.5	52.466	
P1	0.25	44.503	
P1	0.125	43.316	
P1	0.0625	37.647	0.366
P1	0.03125	35.758	µg/Ml
P1	0.01563	35.366	
P1	0.00781	29.801	
P1	0.00391	28.859	
P1	0.00195	-4.950	
P2	1	76.444	
P2	0.5	69.801	
P2	0.25	69.714	
P2	0.125	64.068	
P2	0.0625	60.714	0.016
P2	0.03125	59.845	µg/Ml
P2	0.01563	52.252	
P2	0.00781	40.113	
P2	0.00391	38.728	
P2	0.00195	22.059	
P3	0.5	63.066	
P3	0.25	62.278	
P3	0.125	61.594	
P3	0.0625	61.455	
P3	0.03125	60.886	11.166
P3	0.015625	58.594	µg/Ml
P3	0.007813	54.701	
P3	0.003906	53.097	
P3	0.001953	16.535	
P3	0.000977	10.924	
P4	1	95.318	

P4	0.5	95.037	0.004 µg/Ml
P4	0.25	94.536	
P4	0.125	94.392	
P4	0.0625	92.263	
P4	0.03125	66.666	
P4	0.0153163	60.741	
P4	0.00781	54.113	
P4	0.00391	52.466	
P4	0.00195	7.826	
Acarbose	1	21.405	11.166 µg/mL
	5	33.239	
	10	49.353	
	15	59.829	
	20	73.112	

Quantum Chemical Calculations:

In recent years, quantum chemical calculations have proven to be indispensable tools forelucidating the structure–activity relationships (SAR) of a wide variety of compounds [85].

Among the various computational approaches, Density Functional Theory (DFT) has emerged as one of the most extensively employed methods, owing to its favorable balance between computational cost and high accuracy in predicting molecular properties [86].

Structural and Electronic Properties:

In this study, the optimized molecular geometries of the most stable conformations of $NiPPH_2$ and $ZnTPPH_2$(p-methyl) were obtained using the B3LYP hybrid functional inconjunction with the 6-311++G(d,p) basis set. The resulting geometries are depicted in Figure21 illustrating key structural features and spatial arrangements.

Furthermore, Figure 22 presents the spatial distributions of the frontier molecular orbitals:

the electron-donating characteristics associated with the Highest Occupied Molecular Orbital(HOMO) and the electron-accepting characteristics attributed to the Lowest UnoccupiedMolecular Orbital (LUMO).These frontier orbitals play a crucial role in defining the chemical reactivity and biological activity of the compounds.

The ionization potential (I) was estimated from the negative energy of the HOMO, whilethe electron affinity (A) was derived from the negative energy of the LUMO. The differencebetween these two orbital energies, commonly referred to as the HOMO–LUMO energy gap(ΔE_gap), corresponds to the minimum excitation energy necessary for promoting anelectron from the HOMO to the LUMO. This energy gap serves as an important indicator of molecular from the HOMO to the LUMO. This energy gap serves as an important indicator of molecularchemical stability and reactivity [87] .

Generally, a larger HOMO–LUMO gap signifies greater molecular hardness, enhancedthermodynamic stability, and lower chemical reactivity, whereas a smaller energy gap implies increased chemical softness, higher reactivity, and often correlates with improved biological activities [88] . Thus, analysis of these parameters provides essential insights into the potential behavior of the studied compounds in various chemical and biological environments.

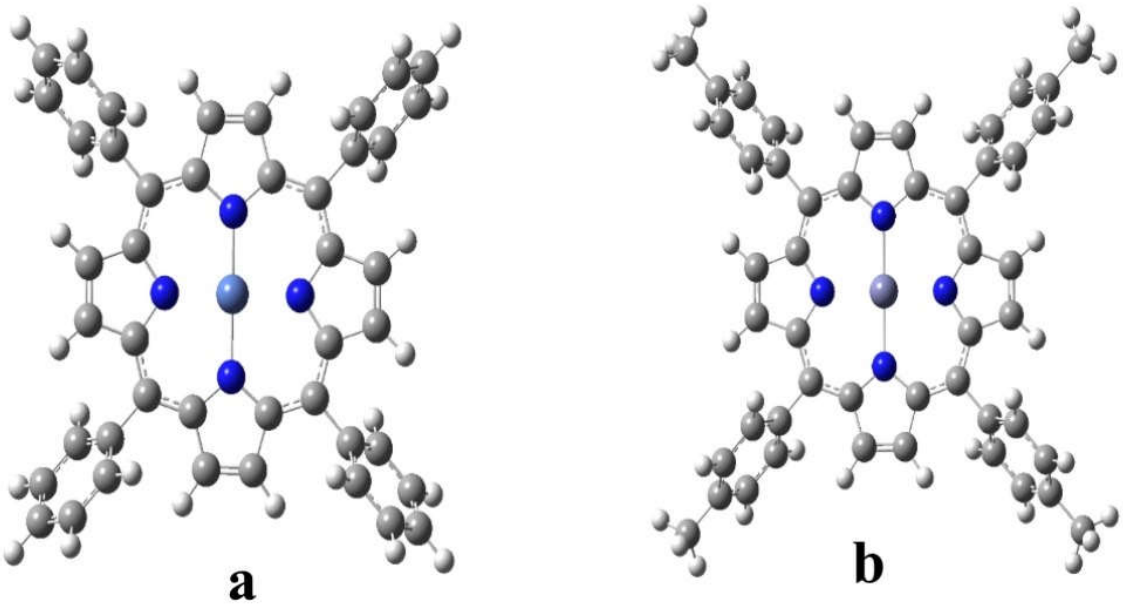

Figure7. Optimized molecular structures of NiPPH 2 (a) and ZnTPPH 2 (p-methyl) (b)

Table3 provides a summary of the chemical reactivity descriptors for the analysed

compounds, which were calculated using density functional theory (DFT). The descriptorsinclude total energy (E), chemical hardness (η), electronic chemical potential (μ), and)electrophilicity (ω

Table 3. Global chemical reactivity descriptors for NiPPH2 and ZnTPPH2(p-methyl)calculated by B3LYP/6- 311++G (d,p)

Quantum parameters	$NiPPH_2$	$ZnTPPH_2$(p-methyl)
$\mathbf{E}_{Tot}$ (eV)	-2081.653	-2135.181
$\mathbf{E}_{HOMO}$ (Hartree)	-0.22041	-0.30255
$\mathbf{E}_{LUMO}$ (Hartree)	-0.21015	-0.23922
$\mathbf{\Delta E}_{GAP}$ (Hartree)	-0.01026	-0.06333
Ionization Energy (**I**)	0.22041	0.30255
Electron Affinity (**A**)	0.21015	0.23922
Electronegativity ($\boldsymbol{\chi}$)	0.21528	0.270885
Chemical Potential ($\boldsymbol{\mu}$)	-0.21528	-0.270885
Chemical Hardness ($\boldsymbol{\eta}$)	0.00153	0.031665
Chemical Softness (**S**)	194.93	31.581
Electrophilicity Index ($\boldsymbol{\omega}$)	15.1456	1.1589
Dipole Moment (Debye)	0.0004	0.1129

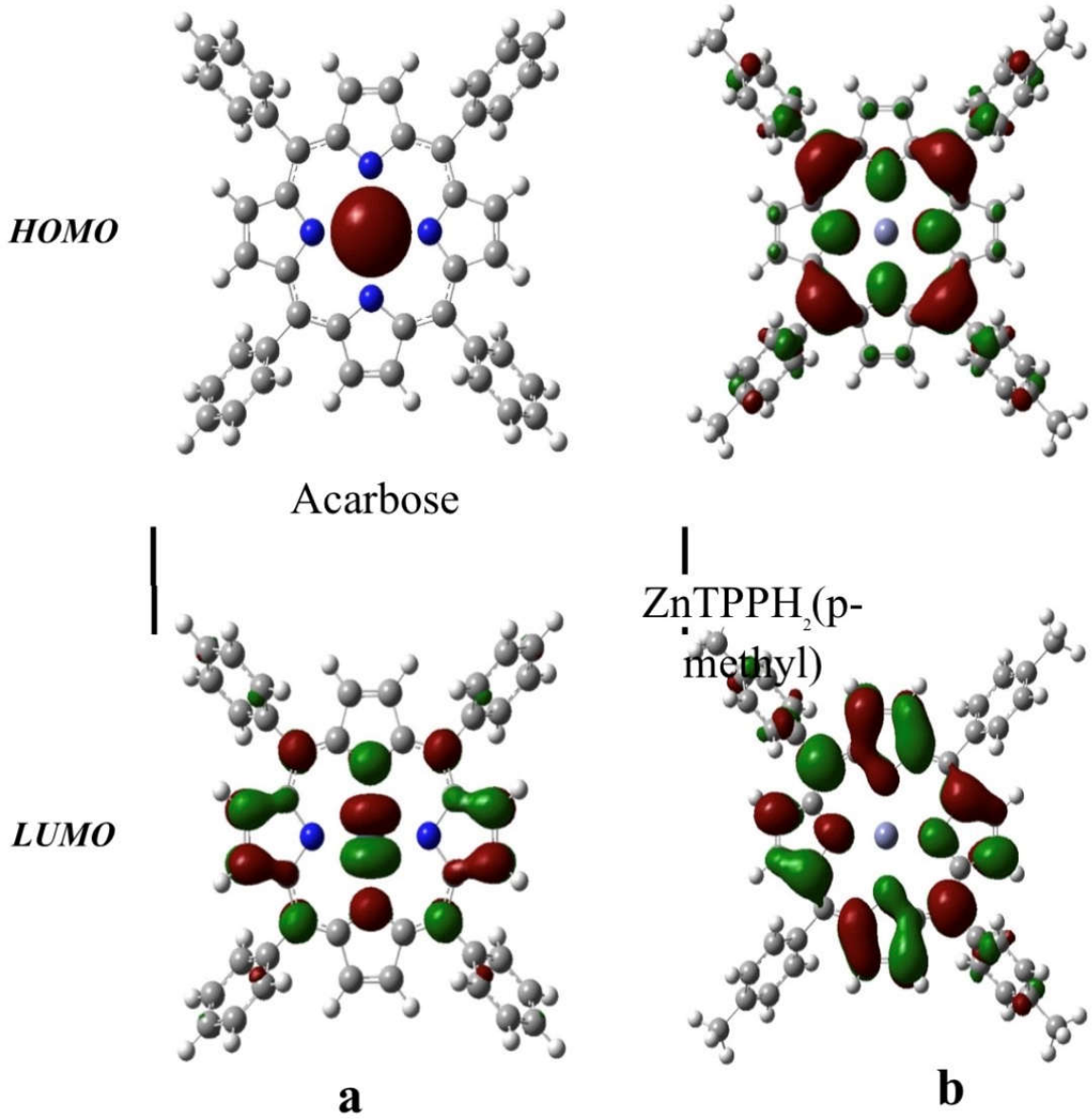

Figure.22 The frontier molecular orbitals density distributions for NiPPH 2 (a) and ZnTPPH 2 (p- methyl) (b)

Table3 displays the energy gap values for NiPPH 2 and ZnTPPH 2 (p-methyl), revealing thatthe energy gap is smaller for both compounds. This suggests that they exhibit good activityand high antioxidant capacity, with the NiPPH 2 compound having the lowest energy gap value of -0.01026 eV. Additionally, the total energy values for the studied compounds (as shown in Table3) indicate that NiPPH 2 has the lowest E Tot value, suggesting that it is less stable than ZnTPPH 2 (p-methyl)

Molecular electrostatic potential surfaces (MEP):

To identify the active sites responsible for electrophilic and nucleophilic attacks, weutilized molecular electrostatic potential surfaces (MEP) as a useful descriptor [89] . The MEPsurfaces provide a three-dimensional visualization of the charge distribution of molecules,which allows for correlation between total charge distribution, dipole moment،electronegativity, partial charges, and sites of chemical reactivity [90] . In Figure23, differentvalues of the MEP are displayed at the surface of the studied acids, with the colours indicating different levels of electron density. In general, the red and yellow colours represent negative regions of the MEP, indicating nucleophilic reactivity, while the blue colour indicates positiveregions corresponding to electrophilic reactivity.

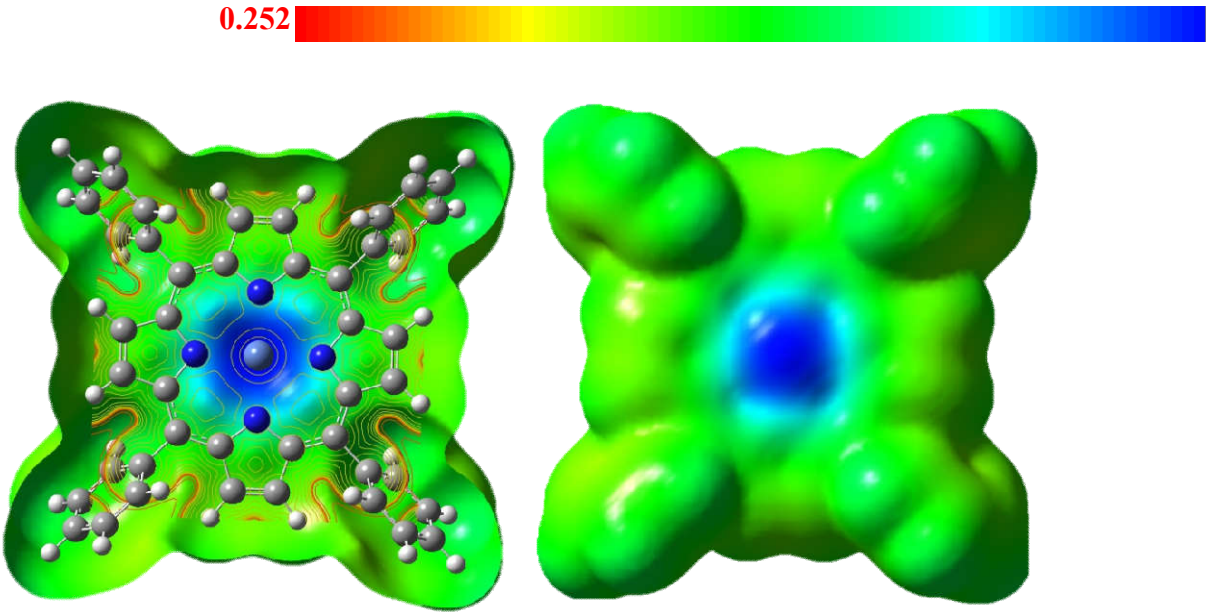

NiPPH$_2$

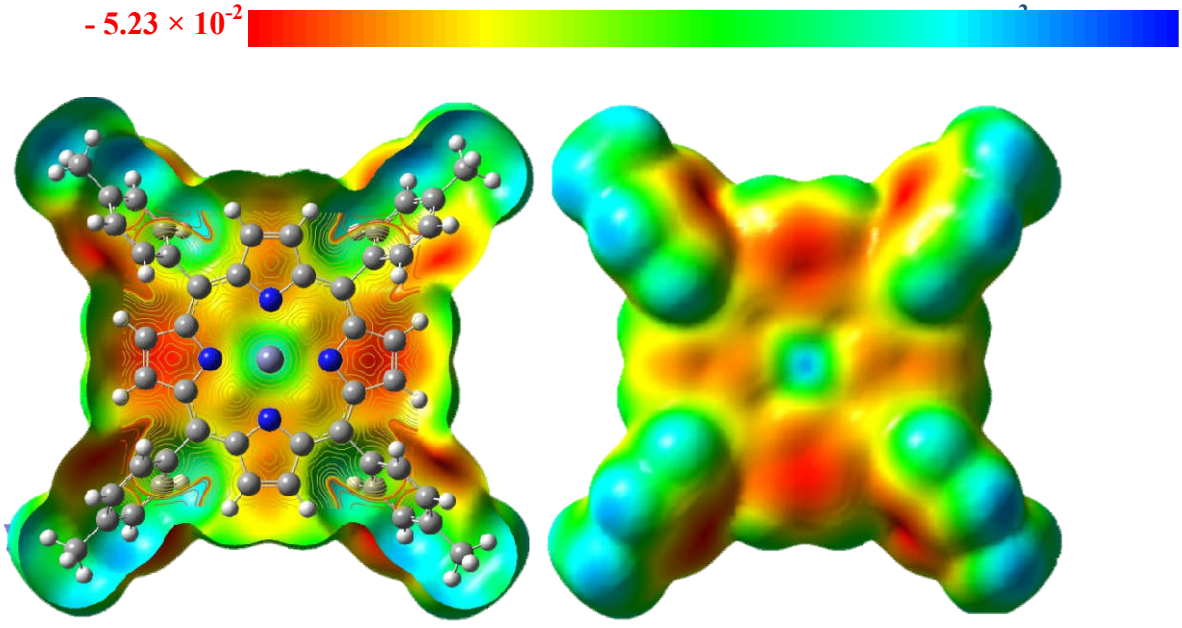

ZnTPPH$_2$(p-methyl)

Figure8: Molecular electrostatic potential of NiPPH 2 and ZnTPPH 2 (p-methy)

The MEP analysis indicates the optimal site for electrophilic attack, which is highlighted inred surrounding the amine functionalities of the ZnTPPH 2 (p-methyl) compound. The metalatoms of both compounds exhibit the highest propensity for nucleophilic attack (as illustrated in Figure23), which may account for their elevated antioxidant activity. Moreover, Figure**23** reveals that NiPPH 2 demonstrates the most negative potential value (- 0.252 a.u.) and th highest positive potentiality value (+ 0.252 a.u).

Cheminformatics Prediction:

PASS Online:

The online tool PASS, standing for Prediction of Activity Spectra for Substances, is readilyaccessible at no cost and is specifically designed to predict the potential biological activitiesof drug-like compounds [91] . Its functionality hinges on an intricate analysis of structure-activity relationships (SAR) within an extensive repository comprising over 300,000 organiccompounds [92] . As such, PASS serves as a pivotal resource for refining chemical synthesisstrategies and guiding the execution of biological assays [93] . In the present investigation،PASS (http://www.way2drug.com/passonline) [91] was employed to forecast the antioxidantand glutathione reductase inhibition activities of NiPPH 2 , ZnTPPH 2 (p-methyl), and acarbose employed as a reference compound), with the findings synthesized in Table4.

Table4: Prediction of antioxidant and glutathione reductase inhibition activity of NiPPH 2,ZnTPPH 2 (p-methyl) and acarbose.

Compound	**Activity/Pa**	
	Antidiabetic	***Alpha-amylase inhibition***
$NiPPH_2$	0.215	0.181
$ZnTPPH_2$(p-methyl)	0.254	0.185
Acarbose	0.253	0.328

The predicted biological activities of $NiPPH_2$, $ZnTPPH_2$(p-methyl), and the referencecompound acarbose were assessed using the PASS online platform, focusing on antidiabeticpotential and alpha-amylase inhibition. The resulting probability scores (Pa) are summarized in Table 4 Among the tested compounds, $ZnTPPH_2$(p-methyl) exhibited the highest predictedantidiabetic activity with a Pa value of 0.254, closely comparable to that of the standard drugacarbose (Pa = 0.253). $NiPPH_2$ also demonstrated a moderate antidiabetic potential (Pa=0.215) although slightly lower than the other two compounds. These findings suggest that $ZnTPPH_2$(p-methyl) could be a promising candidate for antidiabetic applications, potentially rivaling acarbose in terms of predicted bioactivity.

Regarding alpha-amylase inhibition, acarbose, as expected, displayed the highest Pa value‹(0.328).consistent with its established clinical use as an alpha-amylase inhibitor$ZnTPPH_2$(p-methyl) and $NiPPH_2$ showed lower Pa values (0.185 and 0.181, respectively),indicating moderate predicted inhibitory activities. Although these values are inferior toacarbose, they still suggest that both porphyrin derivatives may possess potential- alphaamylase inhibitory effects, meriting further experimental validation.

Overall, these predictive results underline the promising bioactivity profiles of theinvestigated porphyrin compounds, particularly $ZnTPPH_2$(p-methyl), in the context ofantidiabetic therapeutic strategies. The relatively moderate alpha-amylase inhibition scoreshighlight the need for complementary experimental assays to confirm these activities and tooptimize structural features for enhanced efficacy.

Drug-Likeness Prediction:

Drug likeness is conceptualized as a delicate balance of molecular properties and structuralcharacteristics, indicating the degree of similarity between specific compounds andestablished drugs [94] . This assessment is guided by an array of molecule properties,including hydrophobicity, electronic distribution, hydrogen bonding, molecular weight,pharmacophore constituents, bioavailability, reactivity, toxicity, and metabolic stability [95]

One of the widely employed tools for estimating the solubility and permeability ofcompounds, thus predicting their potential as drug candidates, is Lipinski’s rule [96]

According to Lipinski's Rule of 5, compounds with more than five hydrogen bond donors (thesum of NH and OH groups), a molecular weight exceeding 500, a Log P value above 5, andmore than ten hydrogen bond acceptors (the sum of nitrogen and oxygen atoms) are morelikely to experience poor absorption or permeation. The drug likeness properties of Nickeltetraphenyl-porphyrin, Zinc tetra(4-methophenyl)-porphyrin, and acarbose are depicted inTable5, as assessed using the SwissADME server (http://www.swissadme.ch/) [97]

All tested compounds, namely NiPPH 2 , ZnTPPH 2 (p-methyl), and acarbose as a referencedrug, adhere to Lipinski's rule, with their values falling within the normal range. Theassessment of bioavailability indicates that the two compounds under study, NiPPH 2 andZnTPPH 2 (p-methyl), exhibit lower bioavailability compared to the reference drug. Moreover, these compounds fall within the optimal range of physiochemical space, suggesting their potential as lead compounds. Pharmacokinetic analysis reveals similarities between the tested compounds and the reference drug acarbose. This divergence may be attributed to the higher molar refractivity (MR) of NiPPH 2 and ZnTPPH 2 (p-methyl) compared to the reference drug(MR: 198.20 for NiPPH 2 and 221.41 for ZnTPPH 2 (p-methyl) versus 139.27 for the reference drug). In medicinal chemistry, Brenk and pan assay interference compounds (PAINS) structural alerts are employed to predict unstable, reactive, and toxic fragments within thestructure. Notably, both NiPPH 2 and ZnTPPH 2 (p-methyl) exhibit zero alerts in Brenk andPAINS descriptors, further bolstering their potential as viable drug candidates [98]

ADMET Prediction:

The ADMET properties of the compounds NiPPH 2 , ZnTPPH 2 (p-methyl), and the referencedrug acarbose were predicted using the ADMETlab server and the DataWarrior program, with results documented in Tables 6 and7.

Regarding absorption, the investigated porphyrins exhibited superior membranepermeability (Caco-2) compared to the reference drug. Permeability glycoprotein (P-gp)serves as a pivotal drug efflux transporter, regulating drug expulsion from cells to variousbodily compartments, such as the gut lumen, urine, and the brain [99] . Predicted efflux values suggest that all tested antioxidant compounds effectively bypass

the central nervous system(CNS). drug efflux issue, consequently mitigating potential decreases in their bioavailability. suggest that all tested antioxidant compounds effectively bypass the central nervous system(CNS) drug efflux issue, consequently mitigating potential decreases in their bioavailability.Specifically, NiPPH 2 and ZnTPPH 2 (p-methyl) act as inhibitors but not substrates for P-gp, whereas the reference drug functions as both an inhibitor and a substrate. Human Intestinal Absorption (HIA) scores align with qualitative gastrointestinal (GI) absorption descriptors, as predicted by the SwissADME server, indicating lower HIA scores for NiPPH 2 and ZnTPPH 2 (p-methyl) compared to the reference drug.

In terms of distribution, three descriptors were evaluated: Plasma Protein Binding (PPB),Volume Distribution (VD),and Blood–Brain Barrier (BBB) permeability. NotablyZnTPPH 2 (p-methyl), exhibits the highest plasma protein binding,possibly attributed to metalcomplexation enhancing its topological polar surface area (TPSA).Similarly, the volumedistribution (VD) analysis suggests that NiPPH 2 and ZnTPPH 2 (p-methyl) predominantlylocalize within blood components compared to the reference drug.However, the porphyrinderivatives demonstrate limited blood–brain barrier (BBB) penetration, with ZnTPPH 2 (p-methyl) exhibiting the lowest BBB permeabilityThis phenomenon is consistent withprevious studies indicating that excessive hydrogen bonding, facilitated by the metal atom inthe studied compounds, restricts CNS penetration, as observed with certain antihistamines[100]

Regarding metabolism, both NiPPH 2 and ZnTPPH 2 (p-methyl) can be metabolized by theP450 CYP1A2 enzyme, suggesting caution when co-administering lower affinity drugsmetabolized by this enzyme. Similarly, these compounds are susceptible to metabolism byP450 CYP74, a key enzyme involved in the biotransformation of numerous prescribed drugs [101].

Conversely, acarbose, the reference drug, may function as both a substrate and a non-inhibitor for the P450 CYP74 enzyme. Furthermore, NiPPH 2 and ZnTPPH 2 (p-methyl) act asinhibitors but not substrates for the P450 CYP119 enzyme.

In terms of elimination, NiPPH 2 and ZnTPPH 2 (p-methyl) exhibit moderate half-life (T 1/2)durations and low clearance rates (CL) compared to the reference drug, which

displays thehighest T 1/2 values and clearance rates (T 1/2 : 0.018, 0.004, and 0.022 h; CL: 0.447, 0.585, and 8.280 mL/min/kg, respectively).

Table5. Physicochemical, pharmacokinetics, and medicinal chemistry properties of $NiPPH_2$, $ZnTPPH_2$(p-methyl) and acarboseusing SwissADME server

Compound	MW (g/mol)	HBA	HBD	TPSA (Å^2)	Consensus Log Po/w *	MR	GI Absorption	BBB Permeant	P-gp Substrate	Lipinski	Bioavailability Score	PAINS (alert)	Brenk (alert)
$NiPPH_2$	670.693	2	0	34.60	8.69	198.20	Low	No	No	Yes **	0.17	0	0
$ZnTPPH_2$(p-methyl)	733.38	2	0	34.58	8.69	221.41	Low	No	No	Yes **	0.17	0	0
Acarbose	430.71	2	1	29.46	8.27	139.27	Low	No	Yes	Yes **	0.55	0	0

MW: Molecular Weight; HBA: Num. H-Bond Acceptors; HBD: Num. H-Bond Donors; MR: Molar Refractivity; TPSA: Topological Polar Surface Area; GI: Gastrointestinal; BBB: Blood Brain Barrier; P-gp: P Glycoprotein; * Average of five prediction, ** 2 violation: MLOGP > 4.15 and MW>500, PAINS: Pan-assay Interference Compounds.

Table6: Physicochemical, pharmacokinetics, and medicinal chemistry properties of NiPPH 2 , ZnTPPH 2 (p-methyl) and acarbose usingSwissADME server

Compound	Absorption				Distribution			Metabolism; P450 CYP						Elimination	
	Caco-2 p (cm/s)	Pgp (I)	Pgp (S)	HIA	PPB%	VD (L/Kg)	BBB	1A2		74		119		$T_{1/2}$ h	CL mL/min/kg
								I	S	I	S	I	S		
$NiPPH_2$	-5.102	1	0.002	0.009	103.239	0.329	0.016	0.325	0.593	0.896	0.144	0.424	0.006	0.018	0.447
$ZnTPPH_2$(p-methyl)	-5.222	1	0.001	0.004	105.29	0.329	0.003	0.372	0.823	0.831	0.224	0.259	0.013	0.004	0.585
Acarbose	-4.776	0.023	0	0.003	101.24	6.837	0.813	0.068	0.209	0.185	0.932	0.123	0.959	0.022	8.280

PPB (Plasma Protein Binding); VD (Volume Distribution); BBB (Blood–Brain Barrier); T 1/2 (Half Life Time); CL (Clearance Rate); (I); Inhibitor; (S): Substrate

Drug toxicology constitutes a crucial domain in preclinical investigations, as toxicitysignificantly contributes to drug attrition during both discovery and development phases [102].

Consequently, reliable in silico prediction of compound toxicity holds paramount importancefacilitating cost reduction and time-saving in the drug discovery and development processes[103].

The toxicity profiles of the compounds NiPPH 2 , ZnTPPH 2 (p-methyl),and Acarbosewere quantitatively assessed using the Pro-tox-III webserver (https://comptox.charite.de/protox3/) [104] , and qualitatively evaluated via the ADMETlabserver (ADMETlab 2.0 (scbdd.com)) [105] .Results are presented in Table 7

Table4: Toxicity risk assessment of the compounds NiPPH 2 , ZnTPPH 2 (p-methyl) andAcarbose using Pro-tox-III and ADMETlab servers

Compound	**Mutagenicity**	**Cytotoxicity**	**Cardiotoxicity**	**Immunotoxicity**	**Toxicity ***			
					hERG	**H-HT**	**AMES**	**LD_{50} mg/kg**
$NiPPH_2$	None	None	None	None	**--- 0.068**	**+++ 0.953**	**++ 0.711**	**3066**
$ZnTPPH_2$(p-methyl)	None	None	None	None	**--- 0.015**	**-- 0.368**	**-- 0.023**	**3066**
Acarbose	None	None	None	None	**--- 0.028**	**-- 0.358**	**--- 0.001**	**5000**

hERG: Human ether-à-go-go related gene; H-HT: Human Hepatotoxicity; AMES: AmesMutagenicity; LD 50 : Median lethal dose; * calculated by ADMETlab server

From a quantitative perspective, four toxicity descriptors “cardiotoxicity, hepatotoxicity,Ames mutagenicity, and median lethal dose (LD 50) of acute toxicity” were predicted.

Cardiotoxicity, a common side effect arising from off-target interactions between drugs andion channels crucial for cardiac action potential regulation and rhythm control, warrantsattention [106] . Notably, the human ether-a-go-go-related gene (hERG), a potassium ionchannel, is closely associated with severe cardiotoxicity, with hERG blockade being asignificant deterrent in the development of safe pharmaceuticals [107] . Identifying potentialhERG blockers in early drug discovery phases is imperative [106] . Assessment results indicatethat NiPPH 2 and ZnTPPH 2 (p-methyl) exhibit no cardiotoxicity and are the safest among thecompounds analyzed. The elevated cardiotoxicity value of NiPPH 2 is partially attributed to the presence of basic amines in its alkyl chain (hERG: 0.068 for NiPPH 2 vs. 0.028 for acarbose).

Hepatotoxicity and cardiotoxicity are major contributors to drug attrition, with approximately a quarter of marketed drugs withdrawn due to adverse hepatic effects [108] . ZnTPPH 2 (p- methyl) demonstrates hepatic safety, while NiPPH 2 does not. Moreover, the reference drug is predicted to be the least hepatotoxic.

The Ames test, named after its inventor Ames, assesses a compound's mutagenicity thecapacity to induce genetic damage and mutations [109] . Similar to the reference drug‹ZnTPPH 2 (p-methyl) exhibits no mutagenic effects, whereas NiPPH 2 tends to induce geneticdamage and mutations, as predicted by the Ames test. These results diverge from qualitativeresults obtained via the Pro-tox-III webserver, where NiPPH 2 and ZnTPPH 2 (p-methyl) aredeemed non-mutagenic. This discrepancy may stem from differences in the reference models

utilized in both tests. Acute toxicity assessment, expressed as the median lethal dose (LD 50), is pivotal in drug discovery and development [110] . NiPPH 2 and ZnTPPH 2 (p-methyl) display the highest acute toxicity, reflected in their lowest LD 50 values, while the reference drug demonstrates greater safety, with the highest (LD 50 value (LD 50 [mg/kg]: 3066 and 5000, respectively)

Molecular Docking:

A molecular docking study was performed to investigate the inhibitory and binding properties of $NiPPH_2$ and $ZnTPPH_2$(p-methyl) with the enzyme alpha-amylase. Alpha-amylase is a crucial enzyme responsible for the hydrolysis of starch into simpler sugars such as maltose and glucose [111]. Inhibiting alpha-amylase slows carbohydrate digestion and glucoseabsorption, thereby serving as an effective therapeutic strategy for controlling postprandialhyperglycaemia in diabetic patients [112].

Therefore, the inhibition of alpha-amylase has been recognized as an important mechanismfor the development of antidiabetic agents [113] . Molecules that effectively bind to the active site of alpha-amylase and block its activity can help regulate blood sugar levels and mitigate diabetes-related complications.

The molecular docking results indicated that hydrogen bonding, hydrophobic interactions, and π-π stacking played key roles in the binding of the investigated compounds to the active site of alpha-amylase.Figure 24 shows the molecular interactions of $NiPPH_2$, $ZnTPPH_2$(p-methyl), and the reference drug acarbose with the key amino acid residues of alpha-amylaseThe specific interacting residues, types of interactions, and bond distances are detailed inTable 9.

These findings highlight the potential of $NiPPH_2$ and $ZnTPPH_2$(p-methyl) as promisingcandidates for alpha-amylase inhibition, contributing to the development of novel antidiabetic therapies.

Table5: Interaction types between ligands and glutathione reductase (PDB ID: 1HNY)

Compound	H-Bond (Length Å)	Hydrophobic Interactions	π-Cation Interactions	Docking Score (Kcal)
$NiPPH_2$	-	Val 64, Lys 67, Tyr 106, Tyr197, Pro 368, Val 370, Phe 372, Leu 444	Lys 66, Lys 67	-7.25
$ZnTPPH_2$(p-methyl)	-	Tyr 197, Lys 335, Ala 336, Leu 337, Leu 338, Tyr 364, Thr 369	-	-7.33
Acarbose	Asp 441 (1.99)	Lys 66, Ile 198, Leu 338, Pro 340, Pro 368, Thr 369, Val 370, Leu 444, Gln 445	-	-8.16

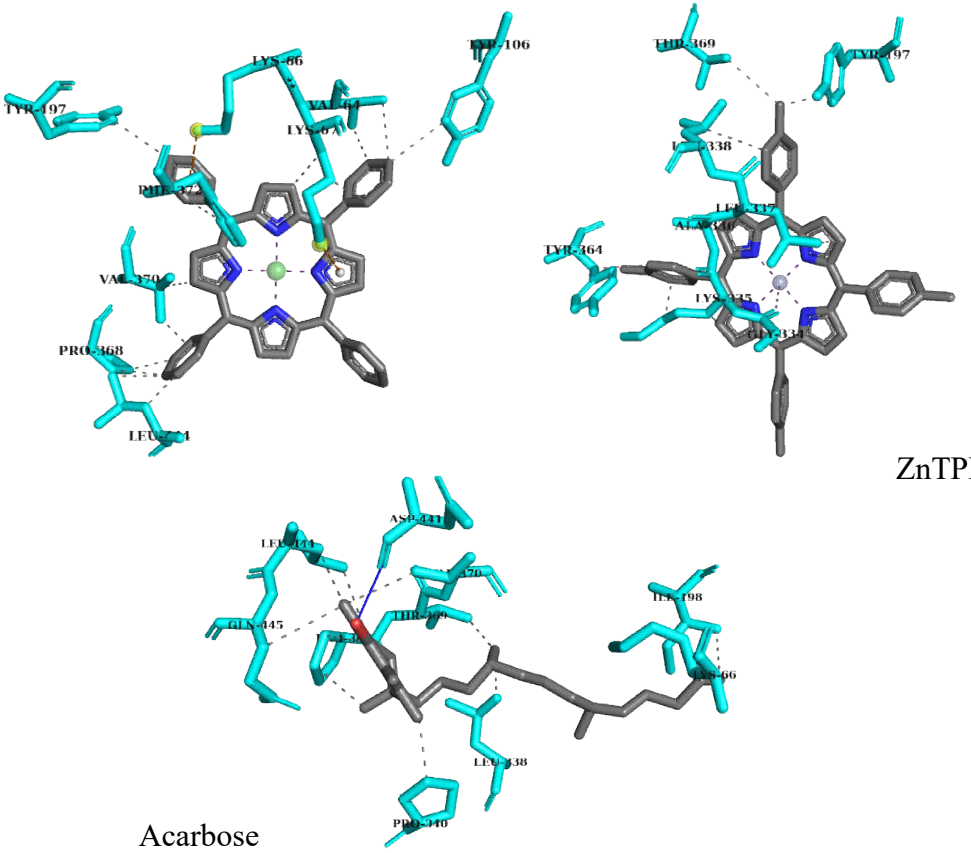

Figure9. Best docking poses for glutathione reductase interacting with NiPPH 2 , ZnTPPH 2 (p- methyl) and acarbose illustrating H-bonds, hydrophobic, and π-cation interactions

The reference inhibitor, acarbose, exhibits the highest docking score of -8.16 kcal/mol,reflecting its strong affinity for the active site of alpha-amylase. In comparison, $NiPPH_2$displays a lower docking score of -7.25 kcal/mol, as detailed in Table 10, suggesting asomewhat weaker but still notable binding interaction.

Unlike acarbose, which forms hydrogen bonds with the enzyme, the compounds $NiPPH_2$and $ZnTPPH_2$(p-methyl) do not engage in hydrogen bonding. Instead, their interactions withthe enzyme are predominantly hydrophobic, involving key amino acid residues such as Val‹64Lys 67, Tyr 106, Tyr 197, Pro 368, Val 370, Phe 372, and Leu 444. These hydrophobicinteractions contribute to the stabilization of the ligand-enzyme complex despite the absence of hydrogen bonds.

In contrast, acarbose establishes a hydrogen bond with Asp 441, where the oxygen atom ofacarbose forms a bond with the hydrogen of Asp 441 at a distance of 1.99 Å. Additionally,$NiPPH_2$ forms two π-cation interactions with Lys 66 and Lys 67, as illustrated in Figure 11,further stabilizing its binding to the active site.

These findings suggest that while $NiPPH_2$ and $ZnTPPH_2$(p-methyl) do not formhydrogen bonds like acarbose, their binding affinity is supported by hydrophobic and π-cation interactions, providing a viable mechanism for alpha-amylase inhibition.

GENERAL CONCLUSION

Conclusion

In conclusion, this study on the effect of porphyrin derivatives as inhibitors of the α-amylase enzyme has shown promising and encouraging results, highlighting the potential of these molecules as effective compounds that could contribute to the development of supportive therapies for blood glucose regulation, especially in diabetic patients. Through laboratory experiments, it was found that compound P4 exhibited the highest inhibitory capacity compared to the other compounds, recording the lowest IC50 value, followed by compound P2, which underscores their potential as lead candidates for the development of natural α-amylase inhibitors.

Additionally, quantum chemical calculations (using the DFT method) and molecular simulations helped understand the electronic and structural properties of these compounds. The results showed that their chemical characteristics align with the observed biological activity. The study also revealed that electronic distribution and interactions with the enzyme's active site play a crucial role in determining the inhibitory efficacy.

Collectively, these findings indicate that targeting carbohydrate-digesting enzymes using porphyrin derivatives may be a promising pathway for developing new drugs capable of improving the management of diabetes, particularly given the increasing need for natural, safe, and effective treatments compared to conventional drugs, which may be associated with undesirable side effects.

Despite the positive results, it is important to emphasize the necessity of continuing this work with additional studies, including the assessment of the acute and chronic toxicity of these compounds, as well as investigating their pharmacokinetic properties such as absorption, distribution, metabolism, and excretion (ADME). Furthermore, preliminary clinical trials are essential to confirm their efficacy and safety in humans.

Advancing in this area will significantly contribute to opening new horizons for the treatment of diabetes by utilizing naturally derived compounds that offer high efficacy and low risk. Therefore, this research represents a first step toward achieving this goal, while emphasizing the importance of ongoing research to complete the full picture regarding the potential clinical application of these compounds.

References

[1]-M. O. Senge, M. Davis, J. Porphyr. Phthalocyanines 2010, 14, 557–567.

[2]- Iovine, P.M., and al., Syntheses and 1H NMR Spectroscopy of Rigid, Cofacially Aligned, Porphyrin− Bridge− Quinone Systems in Which the Interplanar Separations between the Porphyrin, Aromatic Bridge, and Quinone Are Less than the Sum of Their Respective vander Waals Radii. Journal of the American Chemical Society, 2000. 122(36): p. 8717-8727.

[3]-Goff, H. and E. Shimomura, Solution characterization of" intermediate-spin" iron (III) porphyrins by NMR spectroscopy. Journal of the American Chemical Society, 1980. 102(1): p.31-37.

[4]-Zakavi, S., et al., Substitution effects on the UV–vis and 1H NMR spectra of the dications of meso and/or β substituted porphyrins with trifluoroacetic acid: Electron-deficient porphyrins compared to the electron-rich ones. Inorganic Chemistry Communications, 2011. 14(11): p.1827-1832.

[5]-Craig, J., The Porphyrins Handbook, vol. KM Kadish, KM Smith, R. Guilard, 1999.

[6]-Whitlock, H. W.; Bower, K. B. Tetrahedron Lett. 1965, 52, 4827-4831.

[7]- Gouterman, M., Spectra of porphyrins. Journal of Molecular Spectroscopy, 1961. 6: p. 138-163.

[8]- Krausz, P. and C. Giannotti, Etude spectroscopique UV-visible de la complexation de mono et bis-porphyrines de zinc en présence de ligands donneurs. Journal de Chimie Physique, 1983.80: p. 299-303.

[9]- Kobata, K., et al., Synthesis and characterization of dendritic poly (l-lysine) containing porphyrin–fullerene moieties. Synthetic metals, 2007. 157(6-7): p. 311-317.

[10]- KRAUSZ, P., and al. Méthodologie de synthèse pour l’élaboration de photo sensibilisateurs sélectifs à visée anti-cancéreuse.

[11]- D. W. Clack, N. S. Hush, J. Am. Chem. Soc. 1965, 87, 4238–4242.

[12]-R. H. Felton, H. Linschitz, J. Am. Chem. Soc. 1966, 88, 1113–1116.

[13]-R. H. Wopschall, Irving. Shain, Anal. Chem. 1967, 39, 1514–1527.

[14]- J. H. Furhop, K. M. Kadish, D. G. Davis, J. Am. Chem. Soc. 1973, 95, 5140–5147.

[15]-A. Wolberg, J. Manassen, J. Am. Chem. Soc. 1970, 92, 2982–2991.

[16]-G. S. Wilson, Gerald. Peychal-Heiling, Anal. Chem. 1971, 43, 550–556.

[17]-D. Dolphin, R. H. Felton, D. C. Borg, J. Fajer, J. Am. Chem. Soc. 1970, 92, 743–745.

[18]-C. Inisan, J.-Y. Saillard, R. Guilard, A. Tabard, Y. L. Mest, New J. Chem. 1998, 22, 823–830.

[19]- K. M. Kadish, E. Van Caemelbecke, J. Solid State Electrochem. 2003, 7, 254–258.

[20]-A. Brisach-Wittmeyer, S. Lobstein, M. Gross, A. Giraudeau, J. Electroanal. Chem. 2005, 576, 129–137.

[21]-P. Rothemund, A. R. Menotti, J. Am. Chem. Soc. 1941, 63, 267–270.

[22]- A. D. Adler, F. R. Longo, William. Shergalis, J. Am. Chem. Soc. 1964, 86, 3145–3149.

[23]-A. D. Adler, F. R. Longo, J. D. Finarelli, J. Goldmacher, J. Assour, Korsakoff, J Org Chem 1967, 32, 476.

[24]-D. Dolphin, J. Heterocycl. Chem. 1970, 7, 275–283.

[25]-J. S. Lindsey, R. W. Wagner, J. Org. Chem. 1989, 54, 828–836.

[26]-R. G. Geier, J. S. Lindsey, J Org Chem 1999, 64, 1596–1603.

[27]-X. Feng, M. O. Senge, Tetrahedron 2000, 56, 587–590.

[28]-G. R. Geier, J. B. Callinan, P. Dharma Rao, J. S. Lindsey, J. Porphyr. Phthalocyanines 2001, 05, 810–823.

[29]- Markonac, A., Mac Donald, S.F.Can.J.Chem. 1965: p. 43.

[30]- Lindsey, J.S., Acc.Chem.Res. 2010. 311.

[31]- Smith, K.M., Porphyrins and metalloporphyrins. Vol. 9. 1975: Elsevier Amsterdam.

[32]- Tamez Jr, V., An efficient synthesis of heterocycles: An improved solvent effect in the Barton-Zard pyrrole synthesis and a one step synthesis of benzothiazole derivatives. 2006: Texas A&M University-Kingsville.

[33]- Bacton.D.H.R.Zard, S.Z.J.Cem.Soc,chem..Commom, 1935. p. 1098.

(34) OMS. Organisation Mondiale de la Santé. (2016). Rapport mondial sur le diabète

(35)DeFronzo R.A., Ferrannini E., Alberti K.G.M.M., Zimmet P. & Alberti G., (2015).International Textbook of Diabetes Mellitus, 2 volume Set. John Wiley & Sons. p. 1228.

(36) Luka, C., Olatunde, A., Tijjani, H., Olisa-Enewe, I., Luka, C., Olatunde, A.,... Olisa-Enewe, I. (2013). EFFECT OF AQUEOUS EXTRACT OF PHASEOLUS

(37)KRAZA, L. (2021). Evaluation de l'activité antioxydante, antimicrobienne et antidiabétique des composés phénoliques d'une plante médicinale Globularia alypum L. dans la région de Laghouat. 30-35, 65-72

(38)Haffner, S. M. (1998). Epidemiology of type 2 diabetes: riskfactors. Diabetes care, 21 (Supplement3), C3-C6 1987.

(39)Schaefer-Graf, Thomas, B., Anny H, X., Ruth K, P., Siri L, K. S.-G., Thomas, B., ... Siri L,K. (2002). Clinical predictors for a high risk for thedevelopment of diabetes mellitus in the early puerperium in women with recent gestational diabetes mellitus. Departments of Obstetrics and Gynecology, 751-756.

(40)Chaouki, S. (2012). Valorisation d'une plante médicinale à activité antidiabétique de la région de Tlemcen Anacyclus pyrethrum L. Application de l'extrait aqueux à l'inhibition de corrosion d'un acier doux dans H2SO4 0.5M. TLEMCEN: UNIVERSITE ABOUBEKR BELKAID.TLEMCCinerea (L).

(41)AMARA,F, BENGHANEM,Z, 2012. Effet antidiabétique des plantes Médicinales. Mémoier de fin d'étude, Université A. MIRA de Bejaia, Algérie. p. 28

(42)KARURANGA, S. FERNANDES, J. HUANG, Y. MALANDA, B.2017, du Diabète, F.F.I., L'Atlas du Diabète la Huitième édition de la FID, p 150 Brussel.

(43)KEBIR, N. 2018. Propriétés du Lait de chamelle cru sur les profils glucidique et lipidique des rats Wistar rendus diabétiques par l'alloxane.

(44)Pemuter L., Thomas J., (2006). Diabétologie, Affections Métaboliques: Soins Infirmiers.
Ed:Masson Elsevier. Paris. 09. P: 30/172.

(45)favier F, Fianu A, Naty N, Le Moullec N, Papoz L. (2005). Essai de prévention primaire du diabète de type 2 et du syndrome métabolique à la Réunion: Revue Médicale de l'Assurance Médicale. 36): 5-13.s

(46)Arfa L., Abid A., Kéfi R., Nouira S., (2008). Base génétique du ldiabète. XI éme congrès de la Société Tunisienne de médecine interne www.stmi.org.tn. Janvier 2011.

(47)Langlois A., (2008). Optimisation de la revascularisation des ilots pancréatiques au cours de la transplantation, approche génétique ou pharmacologique. Thèse de doctorat . Université Louis Pasteur. Strasbourg. France.

(48)Dubois LD., (2010). Progrés physiopathologiques dans le diabéte de typel. Revue du praticien. Vol.60. P: 165-69.

(49)Carneir M., Dumont C., (2009). Maladie de Biermer chez une adolescente diabétique.

Archive de Pediatrie. Vol.16 (4): 357-59.

(50)Erika F. Brutsaert. (2020). Traitement médicamenteux du diabète sucré. Le manuel MSD.Disponible à (https://www.msdmanuals.com/fr/).

(51)Sinonis-Bik AM, Eekhoff EM, Moor MH, Kramer M, Boosmsma D, Heine RJ. (2010).Gene variants in the novel type 2 diabetes loci CDC123/CAMKID, THADA, ADAMTS9, BCL11A, and MTNRIB affect different aspects of pancreatic beta-cell function. Diabetes. 2010; 59: 293-301

(52)Raverot G. (2005). Diabète sucré de types 1 et 2 de l'enfant et de l'adulte: Edition La Collection Hippocrate. 11-233.

(53)Magnan C, Ktorza A. (2005).Production and secretion of insulin by the pancreatic ß-cell.EMC Endocrinologie. 2: 241-264.

(54)Henri M. (2011). Obésité er insulino-résistance :Etude longitudinale avec un traceur du transport du glucose, le [1251]-6-déoxy-6-iodo D-glucose. Thèse doctorat. Université de Grenoble

(55)Halimi S. (2006). Metformin: 50 years old, fit as a fiddle, and indispensable for its pivotal role in type 2 diabetes management. Diabetes Metabolism. 32:555-6.

(56)SCHLIENGER, J.-L. 2014. Diabète et phytothérapie: les faits. Médecine des maladies Métaboliques, 8, 101-106.

(57)HAMZA, N., BERKÉ, B., CHÈZE, C., AGLI, A., GIN, H. & MOORE, N. 2009Phytothérapie et diabète: plantes hypoglycémiantes les plus utilisées par des sujetsdiabétiques. Recherches sur les Plantes Aromatiques et Médicinales Fees. Maroc, 255-258.

(58)Ehrenkranz, J. R., Lewis, N. G., Ronald Kahn, C., & Roth, J. (2005). Phlorizin: a review. Diabetes/metabolism research and reviews, 21(1), 31-38

(59)Cook D.L., Ikeuchi M. and Fujimoto W.Y. (2000). Lowering of pHi inhibits Ca2+-activatedK+ channels in pancreatic B-cells. Nature. 311(5983): 269-71. Henquin J-C.

(60)Satin L.S., Tavalin S.J. and Smolen P.D.(1994).Inactivation of HIT cell Ca2+ current by a simulated burst of Ca2+ action potentials. Biophys J. 66(1): 141-8.

(61)Duparc Thibaut (2012). Communication inter-organes dans le contrôle du métabolisme glucidique: Mise en évidence de l'implication du monoxyde d'azote et de l'apeline dans l'hypothalamus. Thèse de doctorat. Université Toulouse III - Paul Sabatier. P 7,8,11, 17,18,21,2.

(62)Van Obberghen E., Baron V., Delahaye L., Emanuelli B., Filippa N., Giorgetti-Peraldi S., Lebrun P., Mothe-Satney I., Peraldi P., Rocchi S., Sawka-Verhelle D., Tartare Deckert S. and Giudicelli J. (2001). Surfing the insulin signaling web. Eur J Clin Invest. 31(11): 966-77.

(63)White M.F. (2002). IRS proteins and the common path to diabetes. Am J Physiol Endocrinol Metab. 283(3): E413-22

(64)Saltiel A.R. and Kahn C.R. (2001). Insulin signalling and the regulation of glucose and lipid metabolism. Nature. 414(6865): 799-806.

(65)Burcelin R, Li J, Charron MJ. (1995). Cloning and sequence analysis of the murine glucagon receptor-encoding gene. Gene 164: 305-310.

(66)Wakelam MJ, Murphy GJ, Hruby VJ, Houslay MD (1986). Activation of two signal-transduction systems in hepatocytes by glucagon. Nature 323: 68-71.

(68)Nishide, T., Nakamura, Y., Emi, M., Yamamoto, T., Ogawa, M., Mori, T., Matsubara, K. (1986). Primary structure of human salivary alpha-amylase gene. Gene, 41, 299-304.

(69)PDB, Protein Data Bank. (2008). Human pancreatic alpha-amylase complexed with nitrite.DOI: 10.2210/pdb2QMK/pdb.

(70) Voet, D. & Voet, J. G. (2005). Biochimie. Bruxelles. Editions de Boeck Université. 2ème édition. pp. 1600.

(71) Tormo, M. A., Gil-Exojo, I., de Tejada, A. R., & Campillo, J. E. (2004). Hypoglycaemic and anorexigenic activities of ana-amylase inhibitor from white kidney beans (Phaseolus vulgaris) in Wistar rats. British journal of nutrition, 92(05), 785-790.

(72) Faiveley, M. (2010). Procédés biochimiques et chimiques en agroalimentaire. Produits d'origine végétale. Fabrication des bières. Techniques-ingénieur. ENILBIO poligny. France.

(73) Khacheba, I., Boussoussa, H., Djeridane, A., Bekhaoua, A., Bensayah, N., Yousfi, Khacheba, I., Djeridane, A., Kameli, A., and Yousfi, M.2014.

(74) BERRIHA, A., & BOUKHRIS, A. (2019). Effet des extraits de polysaccharides sur l'inhibition de l'a-glucosidase et de l'a-amylase (Doctoral dissertation, UNIVERSITE KASDI MERBAH-OUARGLA).

[75] M.J. Frisch, G.W. Trucks, H.B. Schlegel, G.E. Scuseria, M.A. Robb, J.R. Cheeseman,J.A. Montgomery Jr, T. Vreven, K.N. Kudin, J.C. Burant, Wallingford CT: Gaussian,Gaussian 16, Revis. C.01. (2004).

[76] B. Miehlich, A. Savin, H. Stoll, H. Preuss, Results obtained with the correlation energydensity functionals of becke and Lee, Yang and Parr, Chem. Phys. Lett. 157 (1989)200–206. https://doi.org/10.1016/0009-2614(89)87234-3.

[77] N. Chafai, S. Chafaa, K. Benbouguerra, D. Daoud, A. Hellal, M. Mehri, Synthesis,characterization and the inhibition activity of a new α-aminophosphonic derivative onthe corrosion of XC48 carbon steel in 0.5 M H2SO4: Experimental and theoreticalstudies, J. Taiwan Inst. Chem. Eng. 70 (2017) 331–344.https://doi.org/10.1016/j.jtice.2016.10.026.

[78] D.A. Filimonov, A.A. Lagunin, T.A. Gloriozova, A. V Rudik, D.S. Druzhilovskii, P. VPogodin, V. V Poroikov, Prediction of the biological activity spectra of organiccompounds using the PASS online web resource, Chem. Heterocycl. Compd. 50 (2014)444–457.

[79] A. Daina, O. Michielin, V. Zoete, SwissADME: A free web tool to evaluatepharmacokinetics, drug-likeness and medicinal chemistry friendliness of smallmolecules, Sci. Rep. 7 (2017) 1–13. https://doi.org/10.1038/srep42717.

[80] S. Kim, P.A. Thiessen, E.E. Bolton, J. Chen, G. Fu, A. Gindulyte, L. Han, J. He, S. He,B.A. Shoemaker, J. Wang, B. Yu, J. Zhang, S.H. Bryant, PubChem substance andcompound databases, Nucleic Acids Res. 44 (2016) D1202–D1213.https://doi.org/10.1093/nar/gkv951.

[81] P.A. Karplus, G.E. Schulz, Substrate binding and catalysis by glutathione reductase asderived from refined enzyme: Substrate crystal structures at 2Å resolution, J. Mol.Biol. 210 (1989) 163–180. https://doi.org/10.1016/0022-2836(89)90298-2.

[82] G.M. Morris, R. Huey, A.J. Olson, UNIT using AutoDock for ligand-receptordocking,Curr. Protoc. Bioinforma. 24 (2008) 8–14.https://doi.org/10.1002/0471250953.bi0814s24.

[83] C. Steffen, K. Thomas, U. Huniar, A. Hellweg, O. Rubner, A. Schroer, AutoDock4 andAutoDockTools4: Automated Docking with Selective Receptor Flexibility, J. Comput.Chem. 31 (2010) 2967–2970.

[84] S. Salentin, S. Schreiber, V.J. Haupt, M.F. Adasme, M. Schroeder, PLIP: Fullyautomated protein-ligand interaction profiler, Nucleic Acids Res. 43 (2015)W443–W447. https://doi.org/10.1093/nar/gkv315.

[85] P. Maitarad, J. Han, D. Zhang, L. Shi, S. Namuangruk, T. Rungrotmongkol, Structure-activity relationships of NiO on CeO2 nanorods for the selective catalytic reduction ofNO with NH3: Experimental and DFT studies, J. Phys. Chem. C. 118 (2014)9612–9620. https://doi.org/10.1021/jp5024845.

[86]H.P. Varbanov, M.A. Jakupec, A. Roller, F. Jensen, M. Galanski, B.K. Keppler,Theoretical investigations and density functional theory based quantitative structure-activity relationships model for novel cytotoxic platinum(IV) complexes, J. Med.Chem. 56 (2013) 330–344. https://doi.org/10.1021/jm3016427.

[87]M. Mehri, N. Chafai, L. Ouksel, K. Benbouguerra, A. Hellal, S. Chafaa, Synthesis,electrochemical and classical evaluation of the antioxidant activity of three α-aminophosphonic acids: Experimental and theoretical investigation, J. Mol. Struct.1171 (2018) 179–189. https://doi.org/10.1016/j.molstruc.2018.05.074.

[88] R.G. Parr, R.A. Donnelly, M. Levy, W.E. Palke, Electronegativity: The densityfunctional viewpoint, J. Chem. Phys. 68 (1977) 3801–3807.https://doi.org/10.1063/1.436185.

[89] S. Chidangil, M.K. Shukla, P.C. Mishra, A molecular electrostatic potential mappingstudy of some fluoroquinolone anti-bacterial agents, J. Mol. Model. 4 (1998) 250–258.https://doi.org/10.1007/s008940050082.

[90] M. Alam, S. Park, Molecular structure, spectral studies, NBO, HOMO–LUMO profile,MEP and Mulliken analysis of 3β, 6β-dichloro-5α-hydroxy-5α–cholestane, J. Mol.Struct. 1159 (2018) 33–45.

[91] D.A. Filimonov, A.A. Lagunin, T.A. Gloriozova, A. V Rudik, D.S. Druzhilovskii, P. VPogodin, V. V Poroikov, Prediction of the biological activity spectra of organiccompounds using the PASS online web resource, Chem. Heterocycl. Compd. 50 (2014)444–457.

[92] A.L. Toppo, M. Yadav, S. Dhagat, S. Ayothiraman, J.S. Eswari, Molecular docking andADMET analysis of synthetic statins for HMG-CoA reductase inhibition activity,(2021).

[93] M.A. Sultan, M.S.A. Galil, M. Al-Qubati, M.M. Omar, A. Barakat, Synthesis,molecular docking, druglikeness analysis, and ADMET prediction of the chlorinatedethanoanthracene derivatives as possible antidepressant agents, Appl. Sci. 10 (2020)7727.

[94] O. Ursu, A. Rayan, A. Goldblum, T.I. Oprea, Understanding drug-likeness, WileyInterdiscip. Rev. Comput. Mol. Sci. 1 (2011) 760–781.

[95] P. Ertl, B. Rohde, P. Selzer, Fast calculation of molecular polar surface area as a sum offragment-based contributions and its application to the prediction of drug transportproperties, J. Med. Chem. 43 (2000) 3714–3717.

[96] C.A. Lipinski, F. Lombardo, B.W. Dominy, P.J. Feeney, Experimental andcomputational approaches to estimate solubility and permeability in drug discovery anddevelopment settings, Adv. Drug Deliv. Rev. 64 (2012) 4–17.https://doi.org/10.1016/j.addr.2012.09.019.

[97] A. Daina, O. Michielin, V. Zoete, SwissADME: A free web tool to evaluatepharmacokinetics, drug-likeness and medicinal chemistry friendliness of smallmolecules, Sci. Rep. 7 (2017) 1–13. https://doi.org/10.1038/srep42717.

[98] R. Brenk, A. Schipani, D. James, A. Krasowski, I.H. Gilbert, J. Frearson, P.G. Wyatt,Lessons learnt from assembling screening libraries for drug discovery for neglecteddiseases, ChemMedChem. 3 (2008) 435–444.https://doi.org/10.1002/cmdc.200700139.

[99] M.L. Amin, P-glycoprotein inhibition for optimal drug delivery, Drug Target Insights. 7(2013) DTI-S12519.

[100] R.C. Young, R.C. Mitchell, T.H. Brown, C.R. Ganellin, R. Griffiths, M. Jones, K.K.Rana, D. Saunders, I.R. Smith, Development of a new physicochemical model for brainpenetration and its application to the design of centrally acting H2 receptor histamineantagonists, J. Med. Chem. 31 (1988) 656–671.

[101] U.M. Zanger, M. Schwab, Cytochrome P450 enzymes in drug metabolism: regulationof gene expression, enzyme activities, and impact of genetic variation, Pharmacol.Ther. 138 (2013) 103–141.

[102] C. Xu, F. Cheng, L. Chen, Z. Du, W. Li, G. Liu, P.W. Lee, Y. Tang, In silico predictionof chemical Ames mutagenicity, J. Chem. Inf. Model. 52 (2012) 2840–2847.

[103] D. Mulliner, F. Schmidt, M. Stolte, H.-P. Spirkl, A. Czich, A. Amberg, Computationalmodels for human and animal hepatotoxicity with a global application scope, Chem.Res. Toxicol. 29 (2016) 757–767.

[104] M.N. Drwal, P. Banerjee, M. Dunkel, M.R. Wettig, R. Preissner, ProTox: A web serverfor the in silico prediction of rodent oral toxicity, Nucleic Acids Res. 42 (2014)W53–W58. https://doi.org/10.1093/nar/gku401.

[105] J. Dong, N.N. Wang, Z.J. Yao, L. Zhang, Y. Cheng, D. Ouyang, A.P. Lu, D.S. Cao,Admetlab: A platform for systematic ADMET evaluation based on a comprehensivelycollected ADMET database, J. Cheminform. 10 (2018) 1–11.https://doi.org/10.1186/s13321-018-0283-x.

[106] S. Kalyaanamoorthy, K.H. Barakat, Development of safe drugs: the hERG challenge,Med. Res. Rev. 38 (2018) 525–555.

[107] M.L. Ponte, G.A. Keller, G. Di Girolamo, Mechanisms of drug induced QT intervalprolongation, Curr. Drug Saf. 5 (2010) 44–53.

[108] Y. Low, T. Uehara, Y. Minowa, H. Yamada, Y. Ohno, T. Urushidani, A. Sedykh, E.Muratov, V. Kuz'min, D. Fourches, Predicting drug-induced hepatotoxicity usingQSAR and toxicogenomics approaches, Chem. Res. Toxicol. 24 (2011) 1251–1262.

[109] B.N. Ames, J. McCann, E. Yamasaki, Methods for detecting carcinogens and mutagenswith the Salmonella/mammalian-microsome mutagenicity test, Mutat.Res.;(Netherlands). 31 (1975).

[110] T. Lei, Y. Li, Y. Song, D. Li, H. Sun, T. Hou, ADMET evaluation in drug discovery:15. Accurate prediction of rat oral acute toxicity using relevance vector machine andconsensus modeling, J. Cheminform. 8 (2016) 1–19.

[111] H. Laraoui, E. Lanez, N. Zegheb, A. Adaika, T. Lanez, M. Benkhaled, Anti-DiabeticActivity of Flavonol Glucosides From Fumana montana Pomel: In vitro Analysis, InSilico Docking, ADMET Prediction, and Molecular Dynamics Simulations,ChemistrySelect. 8 (2023) e202204512. https://doi.org/10.1002/slct.202204512.

[112] L. ZERROUK, L. BECHKI, E. LANEZ, T. LANEZ, Synthesis, characterization, cyclicvoltammetry, and molecular docking studies of the antioxidant activities of superoxideanion radicals towards meso-tetramethophenyl-porphyrin and meso-tetrabiphenyl-porphyrin, Not. Sci. Biol. 16 (2024) 11823. https://doi.org/10.55779/nsb16211823.

[113] V.N. Toan, N.D. Thanh, L.T. Huyen, N.T. Hanh, D.S. Hai, H.H. Anh, N.T.K. Giang,H.T.K. Van, Design, Synthesis, α-Amylase/α-Glucosidase Inhibition Assay, Induced FitDocking Study of New Hybrid Compounds Containing 4H-Pyrano[2,3-d]pyrimidine,1H-1,2,3-Triazole and D-Glucose Components, Chem. Biodivers. 19 (2022)e202200680. https://doi.org/10.1002/cbdv.202200680.